Ph. D. Thesis

IONOTROPIC GLUTAMATE ANTAGONISM IN THE 4-AMINOPYRIDINE RAT CONVULSION MODEL: THE MORPHOLOGICAL AND FUNCTIONAL ASPECTS OF THE ACUTE SEIZURE

Roland Weiczner M.D.

Experimental and Clinical Neuroscience Doctoral Programme
Doctoral School of Clinical Medicine

Supervisor: Prof. András Mihály M.D., Ph.D., D.Sc.

Department of Anatomy, Histology and Embryology
Faculty of Medicine
University of Szeged

Szeged

2009

LIST OF *IN EXTENSO* PUBLICATIONS RELATED TO THE THESIS

I. Szakács, R., **Weiczner, R.**, Mihály, A., Krisztin-Péva, B., Zádor, Zs., Zádor, E.: Non-competitive NMDA receptor antagonists moderate seizure-induced *c-fos* expression in the rat cerebral cortex. *Brain Res Bull 59: 485-493, 2003* ***IF: 1.943***

II. Kovács, A., Mihály, A., Komáromi, Á., Gyengési E., Szente, M., **Weiczner**, **R.,** Krisztin-Péva, B., Szabó, Gy., Telegdy, Gy.: Seizure, neurotransmitter release, and gene expression are closely related in the striatum of 4-aminopyridine-treated rats. *Epil Res 55: 117-129, 2003* ***IF: 2.377***

III. Mihály, A., Borbély, S., Világi, I., Détári, L., **Weiczner, R.**, Zádor, Zs., Krisztin-Péva, B., Bagosi, A., Kopniczky, Zs., Zádor, E.: Neocortical c-fos mRNA transcription in repeated, brief, acute seizures: Is *c-fos* a coincidence detector? *Internat J Mol Med 15(3): 481-486, 2005* ***IF: 1.847***

IV. Fabene, P. F., **Weiczner, R.**, Marzola, P., Nicolato, E., Calderan, L., Andrioli, A., Farkas, E., Süle, Z., Mihály, A., Sbarbati, A.: Structural and functional MRI following 4-aminopyridine-induced seizures: a comparative imaging and anatomical study *Neurobiol Dis 21: 80-89, 2006* ***IF: 4.377***

V. **Weiczner, R.**, Krisztin-Péva, B., Mihály, A.: Blockade of AMPA-receptors attenuates 4-aminopyridine seizures, decreases the activation of inhibitory neurons but is ineffective against seizure-related astrocytic swelling *Epil Res 78(1): 22-32, 2008* ***IF: 2.377***

VI. Zádor, Zs., **Weiczner, R**, Mihály, A.: Long-lasting dephosphorylation of connexin 43 in acute seizures is regulated by NMDA receptors, in the cerebral cortex of the rat *Mol Med Rep 5(1): 721-727, 2008* ***IF: -***

CIF = 12.921 (ISI JCR 2007)

LIST OF CITABLE ABSTRACTS RELATED TO THE THESIS

I. Mihály, A., **Weiczner, R.**, Krisztin-Péva, B., Dobó, E., Szakács, R., Czigner, A., Zádor, Zs., Bakota, L., Tóth, G.: Seizure-dependent expression of *c-fos* in neurons of the rat hippocampus. *Neurobiology, 9: 339-340, 2001*

II. A. Mihály, **R. Weiczner**, B. Krisztin-Péva, E. Dobó, Zs. Zádor: Seizure-dependent expression of *c-fos* in neurons of the rat cerebral cortex. *It Jour Anat Embr 107: 15, 2002*

III. Bakos M., Krisztin-Péva B., **Weiczner R.**, Mihály A.: Die Veränderungen der Krampfbereitschaft während der postnatalen Entwicklung: immunhisto-chemische Untersuchungen in der Ratte. *Verhandlungen der Anatomischen Gesellschaft, 99. Versammlung in Wien, Suppl. Ann. Anat. 186:78, 2004*

IV. **Weiczner R.**, Mihály A., Krisztin-Péva B.: The AMPA-antagonist GYKI 52466 moderates the seizure-induced *c-fos* gene expression in the rat cerebral cortex. *Verhandlungen der Anatomischen Gesellschaft, 100. Versammlung in Leipzig, Suppl. Ann. Anat. 187:189, 2005*

V. **R. Weiczner**, A. Mihály, S. Borbély, I. Világi, L. Détári, Zs. Zádor, B. Krisztin-Péva, A. Bagosi, Zs. Kopniczky and E. Zádor: Neocortical *c-fos* mRNA transcription in repeated, brief, acute seizures: Is *c-fos* a coincidence detector? *Clinical Neuroscience Suppl.: Abstracts of XI. MIT Congress, Pécs, 2005.*

VI. **Weiczner R.**, Mihály A., Krisztin-Péva B.: The concentration-dependent neo- and allocortical effect of GYKI 52466 in the 4-aminopyridine-induced acute rat seizure model. *Acta Biologica Szegediensis 51 (Suppl 1):56, 2007*

LIST OF ABBREVIATIONS

4-AP	4-aminopyridine
ADC	apparent diffusion coefficient
AMPA	α-amino-3-hydroxy-5-methyl-4-isoxazol propionate
ANOVA	analysis of variance
AOI	area of interest
AQP4	aquaporin-4
BBB	blood-brain-barrier
CA	cornu Ammonis
DMSO	dimethyl-sulphoxide
DWI	diffusion-weighted imaging
EEG	electroencephalography
EM	electron microscopy
EPSP	excitatory postsynaptic potential
FOV	field of view
G	gauss (non-SI unit of magnetic field)
GABA	γ-amino-butyric acid
GAR	goat-anti-rabbit (antibody)
GLU	glutamate
GTCS	generalised tonic-clonic seizure
HPCD	2-hydroxypropyl-β-cyclodextrin
i.d.	internal diameter
i.p.	intraperitoneal
IEG	immediate early gene
IPSP	inhibitory postsynaptic potential
IR	immunoreactive
ITF	inducible transcription factor
LEG	late effector gene
fMRI	functional magnetic resonance imaging
NMDA	N-methyl-D-aspartate
PAP	peroxidase-anti-peroxidase
PBS	phosphate-buffered saline
PCR	polymerase chain reaction
PDS	paroxysmal depolarisation shift
PK	protein kinase

LIST OF ABBREVIATIONS (contd.)

PV	parvalbumin
RARE	rapid acquisition-rapid enhancement
rCBF	regional cerebral blood flow
rCBV	regional cerebral blood volume
ROI	region of interest
SE	status epilepticus
SEM	standard error of the mean
STA-PER	streptavidin peroxidase
T	tesla (SI unit of magnetic field)
T2	transverse relaxation time
T2W	T2-weighted (imaging)
TE	echo time
TR	repetition time
USPIO	ultrasmall superparamagnetic iron oxide
vs.	versus

CONTENTS

1. INTRODUCTION

1.1 The 4-AP acute convulsion model

The excessive, pathologic oversynchronisation *(Perreault and Avoli, 1991; Yang and Benardo, 2002)* of neuronal activity and the disequilibrium between certain excitatory and inhibitory factors *(Gulyás-Kovács et al., 2002; Schwaller et al., 2004)* are considered as the pathophysiologic basis of the epileptiform activity in the central nervous system. The conventional therapeutic regimes concentrate on the strengthening of the inhibitory neurotransmission *(Lukasiuk and Pitkänen, 2000; Holtkamp and Meierkorp, 2007)* whereas the inhibition of the excitatory responses is under current research, but results are mainly available about the role of NMDA (N-methyl-D-aspartate)-mediated events *(Conti and Weinberg., 1999; Borowicz et al., 2001; Szakács et al., 2003)*.

One of the well-known *(Mihály et al., 1990; Peña and Tapia, 2000)* chemical means to elicit acute seizures with generalised tonic-clonic features ***(Fig. 1)*** in an *in vivo* animal model is the 4-aminopyridine (4-AP), having well-circumscribed pharmacokinetic *(Lemeignan et al., 1984; Berger et al., 1989)* and pharmacodynamic *(Perreault and Avoli, 1991; Mihály et al., 2000)* properties; including the cases of human toxicity *(Spyker et al., 1980)* and the contradictory results to introduce this very compound in certain fields of human disease therapy *(Jones et al., 1983; Andreani et al., 2000)*. 4-AP is a nitrogen-containing heterocyclic K^+-channel blocker, exerting its effect mainly via IK(A) and IK(V) channel types *(Brückner and Heinemann, 2000)*, thus the shift of the membrane potential towards depolarisation enables Ca^{2+}-influx ***(Fig. 2)***; mainly via voltage-gated Ca^{2+}-channels and the NMDA receptor ion channels *(Greenberg and Ziff, 2001)*, the latter are opened by the mainly presynaptically acting 4-AP-induced membrane-depolarisation *(Yang and Benardo, 2002)*. The sustained, repeated, synchronised neuronal discharge, the so-called “burst firing” is a basic feature of the central nervous system seizure mechanism *(Labiner et al, 1993)*. The prolonged neuronal depolarisation stimulates both excitatory and inhibitory neurotransmitter release *(Versteeg et al., 1995)*, especially glutamate (GLU) *(Peña and Tapia, 1999; Kovács et al., 2003)* and reinforces the inhibitory (IPSPs) and excitatory postsynaptic potentials (EPSPs) *(Perreault and Avoli, 1991)*. On the basis of the electrophysiological investigations *(Yang and Benardo, 2002)*, one of the 4-AP-induced cortical spontaneous discharge component can be blocked by glutamate receptor antagonists, whereas the other type by $GABA_A$ receptor antagonists, suggesting that it was produced by the synchronisation of GABAergic (GABA, γ-amino-butyric acid) interneurons.

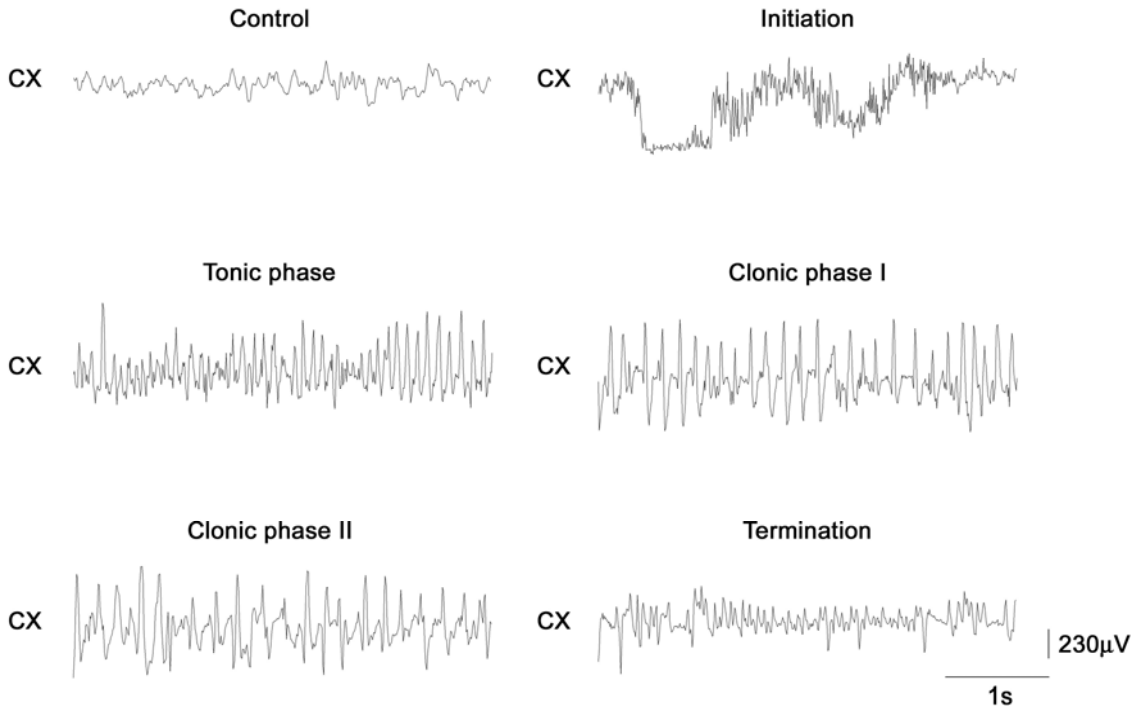

	Duration of first seizure (sec)	Duration of first tonic phase (sec)	Duration of first clonic phase (sec)	Duration of second seizure (sec)	Duration of second tonic phase (sec)	Duration of second clonic phase (sec)	Frequency in tonic phases (Hz)	Frequency in clonic phases (Hz)
Mean (n=5)	53.53	7.38	46.15	73.44	8.96	64.48	7.77	5.23
SD	4.21	4.10	5.12	13.94	5.26	15.30	1.21	0.98

Fig. 1: The EEG appearance of the 4-AP-induced seizure *(Mihály et al., 2005)*. Time and voltage scales are shown. For EEG registration, stainless steel screw-electrodes were implanted over the somatosensory cortex (trunk and hindlimb regions) according to stereotaxic coordinates. An additional screw electrode over the cerebellum served as reference. Following a 10-day-recovery period, the electrodes were connected to the recording instrument. During the 8-hour-recording period, two seizures were detected in each animal except one, in which three events occurred. The convulsions appeared during the first hour of the observation. The first seizure activity appeared on the EEG with an average latency of 20.70±6.48 min. This event was followed by a second seizure, and the mean delay between the two seizure events was 16.22±4.86 min. The mean duration of the first discharges was 53.53±4.21 sec, while the second was significantly lower, lasting for 73.44±13.94 sec. Repetitive spikes characterised each seizure event in the so-called tonic phase and repetitive spikes at a smaller frequency, as well as pike-and-wave complexes in the so-called clonic phase. The EEG seizure did not last over 1 h.

According to our microdialysis investigations *(Kovács et al., 2003)*, fast and highly significant elevation can be demonstrated in the striatal concentration of GLU. Since many of the excitatory afferents of the striatum originate from the cerebral cortex (and thalamus), we may suppose that the elevation in the striatal GLU is consequence of neocortical hyperactivity and the excessive release of the transmitter from corticostriatal (and thalamostriatal) axon terminals. Interestingly, the GLU level reaches its maximum at 120 min, well after the cessation of the electrographic seizure. This explains the long-lasting spiking activity on the striatal EEG and raises the possibility that besides the

postsynaptic depolarization, GLU might regulate the release of other transmitters through metabotropic GLU receptors *(Pisani et al., 2002)*. Recent experimental evidence proves that protein kinase C (the activation of which is coupled to metabotropic GLU receptors) is an important mediator of the phosphorylation of transcription factors which are responsible for *c-fos* gene expression *(Choe and Wang, 2002)*; so, metabotropic receptors themselves can participate in the induction of *c-fos* expression.

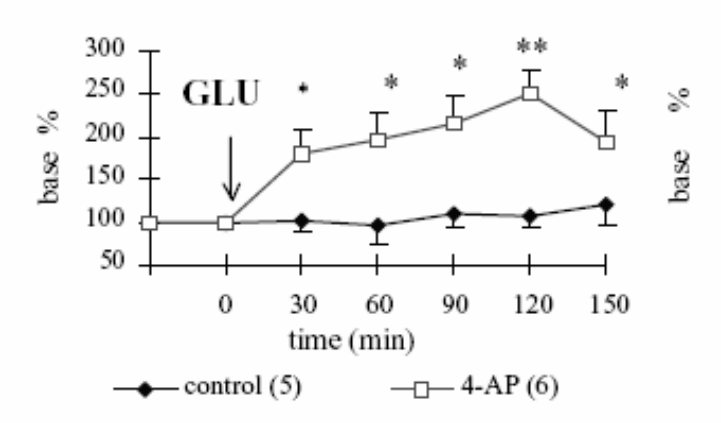

Fig. 2: Changes in concentration of glutamate (GLU) in control and 4-AP-treated rat striatum, expressed as percentages of the basal level *(Kovács et al., 2003)*. The number of dialysis samples (4–6) is given in brackets, and the injection of 4-AP or physiological saline is indicated by arrows. Asterisks denote significant differences: * $p < 0.05$;** $p < 0.01$.

1.2 The immediate-early gene c-fos

The immediate early gene (IEG) *c-fos* *(Morgan and Curran, 1991)* is an inducible transcription factor (ITF) *(Herdegen and Leah, 1998)* playing important role in certain nuclear regulative processes *(Dragunow et al., 1989)*. The gene products of the IEGs, via transcriptional regulation influence the genes (LEGs: late effector genes) involved in the maturation and adaptation mechanisms of the nervous system *(Retchkiman et al., 1996; Schmoll et al., 2001)*, or in plasticity and neurodegeneration *(Herdegen and Waetzig, 2001)*, as well as in epilepsy *(Gass et al., 1992; Rocha et al., 1999)*. The full spectrum of the genes regulated by *c-fos* is not known as a whole *(Ziołkowska et al., 1998; Gebhart et al., 2002)*. Nevertheless, the signal transduction characteristics and the intracellular pathways ***(Fig. 3)*** of *c-fos* gene expression are basically understood *(Blendy et al., 1995; Perkinton et al., 1999; Zirpel et al., 2000; Hardingham et al., 2001)*. The *c-fos* mRNA transcription shows strict correlation with the electrophysiologically proven cellular activity *(Labiner et al., 1993)*, and this correspondence establishes the *Fos* protein (appearing in the cell nuclei of the neurons concerned) as a sensitive marker of the increase of neuronal activity *(Hoffman and Lyo, 2002)*. NMDA and AMPA receptors are amongst the external signals, which activate *c-fos* transcription *(Herdegen and Leah, 1998)*.

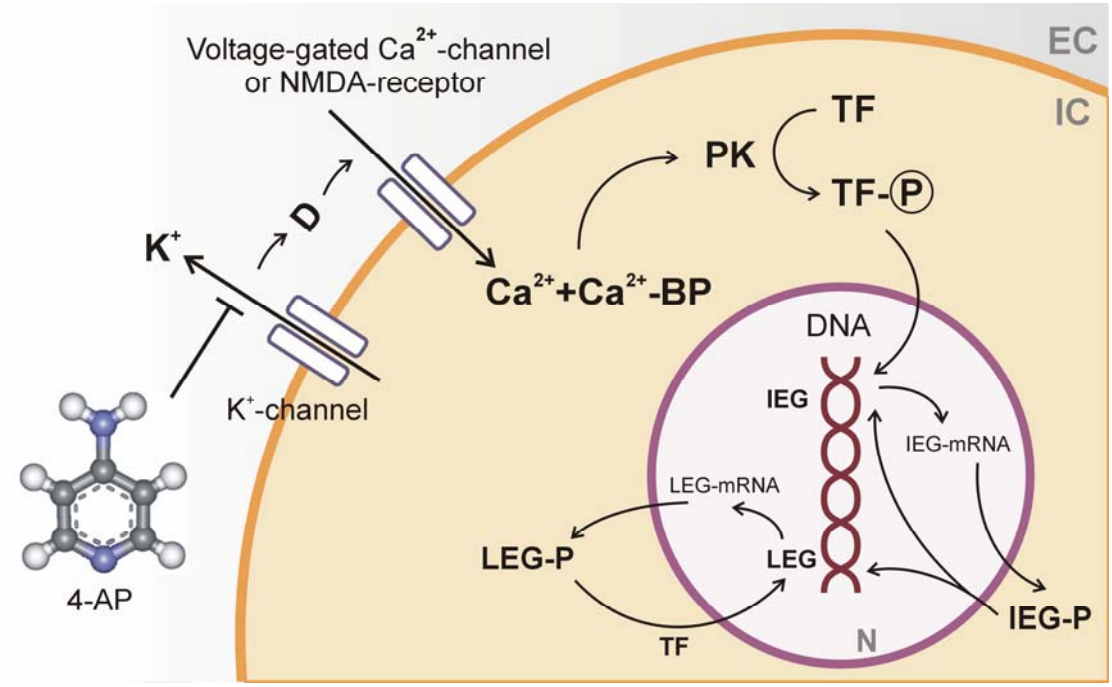

Fig. 3: The signal transduction cascade induced by 4-AP. *Abbreviations:* D-depolarisation; BP-binding protein; PK-protein kinase; TF-transcription factor; P with circle: phosphorylated; IEG-immediate early gene; IEG-P-immediate early gene protein; LEG-late effector gene; LEG-P-late effector gene protein; mRNA-messenger ribonucleic acid; N-nucleus; EC-extracellular space; IC-intracellular space. (*Modified after Dragunow et al., 1989).*

1.3 The astrocytic swelling in seizure

Amongst the earliest neuropathological changes in seizure activity *(Kelso and Cock, 2004)*, the swelling of the astrocytic processes has already been observed *(Fujikawa et al., 1992; Fabene et al., 2006)*. Astrocytes are the main cell types that swell in cytotoxic brain oedema *(Kimelberg, 2004)*, especially the pericapillary foot processes, which are the predominant sites of aquaporin-4 (AQP4) expression in the brain *(Papadopoulos and Verkman, 2007)*. Glutamate, at similar concentrations required to induce neuronal cell death, has been shown to increase cell volume in cultured astrocytes *(Han et al., 2004)*. The astrocytic swelling has numerous deleterious secondary effects, such as the release and decreased uptake of excitatory amino acids *(Kimelberg, 2004)*; worsening the micro-environmental circumstances like a *circulus vitiosus* process. Pharmacological inhibition of seizure activity decreases brain oedema in different animal models *(Clifford et al., 1990; Tian et al., 2005)*. Beside the electron microscopic investigations, the importance of the *in vivo* imaging techniques, such as functional magnetic resonance imaging is continuously increasing *(Blumenfeld, 2007)*.

1.4 The glutamate-receptor antagonists

Studies involving intracellular recording in rat neocortical slices have shown that NMDA receptors contribute to the process of stimulus-induced paroxysmal depolarisation shift (PDS) amplification by prolonging the duration and reducing the latency of the epileptiform discharge *(Hwa and Avoli, 1991)*. The high-affinity open-channel NMDA receptor blocker dizocilpine maleate (MK-801) ***(Fig. 4)*** is also potent anticonvulsant *(Lojková et al., 2006)* and protects against seizure-related brain damage *(Clifford et al., 1990)*. The MK-801 is widely used for NMDA receptor mapping in imaging studies *(Biegon et al., 2007)*; or to establish an experimental schizophrenia in animal models *(Abekawa et al., 2007).*

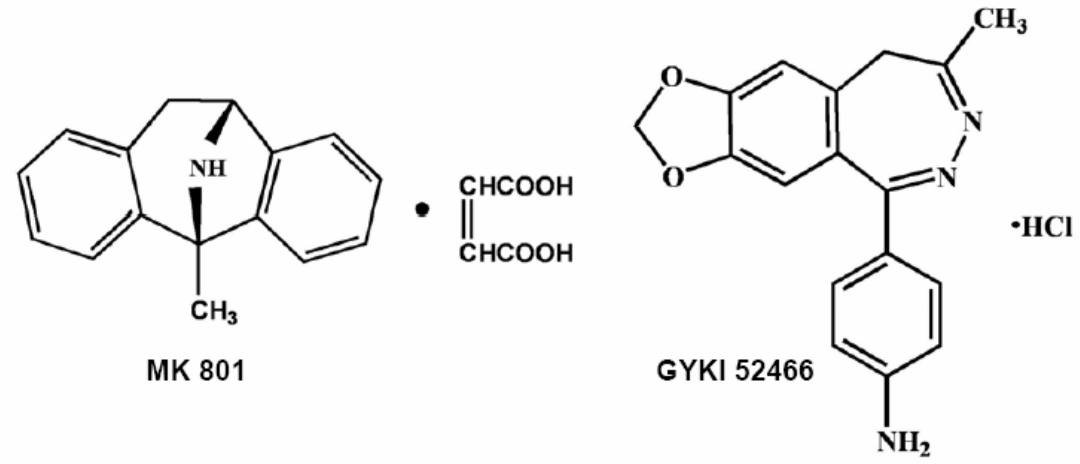

Fig. 4 The chemical structure of the applied glutamate-receptor antagonists.

The compound GYKI 52466 (1-(4-aminophenyl)-4-methyl-7,8-methylenedioxy-5H-2,3-benzodiazepine hydrochloride) ***(Fig. 4)*** is a selective, non-competitive, presumably allosteric antagonist of the AMPA (α-amino-3-hydroxy-5-methyl-4-isoxazol propionate)-subtype ionotropic glutamate receptors *(Donevan and Rogawski, 1998; Arai, 2001)*; with good blood-brain-barrier (BBB) permeability *(Barna et al., 2000)*, neuroprotective effects in seizure and cerebral ischaemia *(Szabados et al., 2001; Arias et al., 1999)*, antinociceptive and anti-inflammatory properties *(Székely et al., 1997; Szabados et al., 2001)* and has other advantageous effects in ischaemic conditions *(Block et al., 1996; Arias et al., 1999)*. Electrophysiological investigations *(Paternain et al., 1995; de Sarro et al., 1995)* proved the antagonistic activity of GYKI 52466 upon the AMPA and kainite receptors, whereas practically no effect has been demonstrated on the NMDA receptors, metabotropic glutamate receptors, and on the $GABA_A$-receptors. According to the kinetic analysis of AMPA receptors, the most likely way of GYKI 52466 effect is elongating the desensitisation-resensitisation process, the channel closing frequency and the deactivation *(Arai, 2001)*.

Synapses in cerebral cortex and hippocampus commonly coexpress NMDA and AMPA receptors *(Nusser, 2000)*. According to this observation, the proconvulsive feature of glutamate-receptor agonists *(Hou et al., 1997; Obrenovitch and Urenjak, 1997)*; and the anticonvulsive effect of the glutamate-receptor antagonists have been proved in several *in vivo* *(Czuczwar et al, 1995; Szakács et al., 2003)* and *in vitro* *(Dóczi et al., 1999; Gulyás-Kovács et al., 2002)* models of experimental epilepsy.

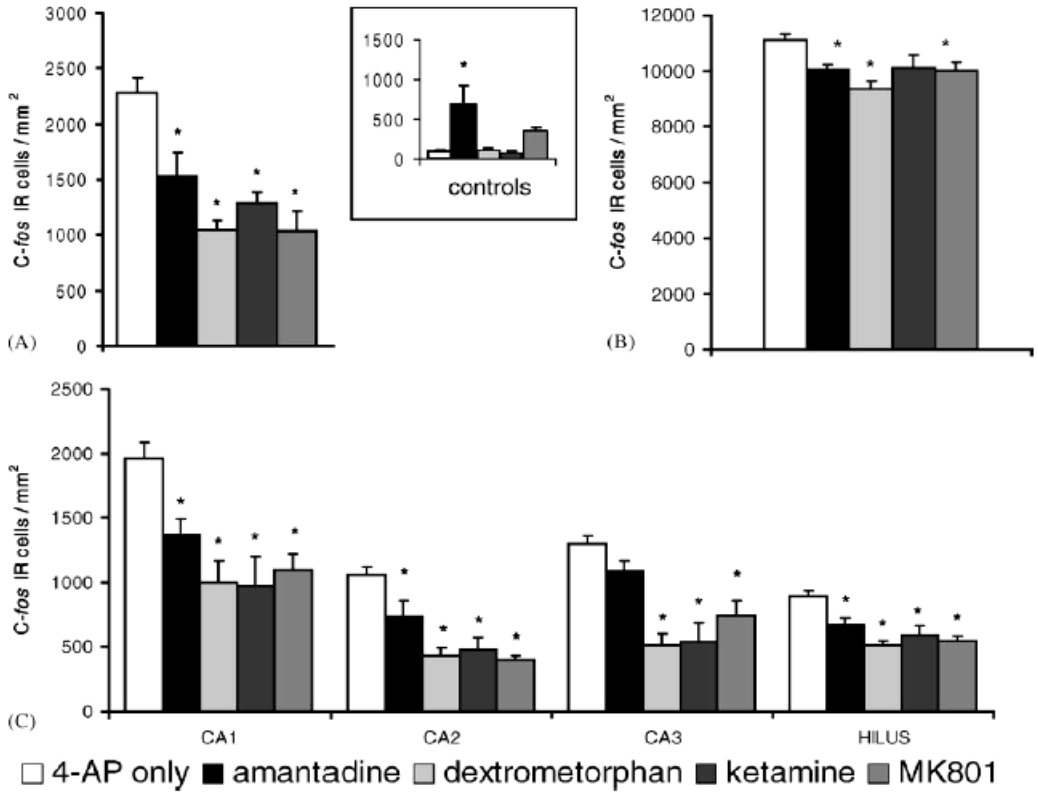

Fig. 5. Quantitative evaluation of Fos-positive cells in the different experimental groups. *(Szakács et al., 2003)* **(A)** results of cell counts in the neocortex in amantadine-, dextrometorphan-, ketamine- or MK-801-pretreated animals, compared with rats injected only with 4-AP. The results of cell counts in the neocortex of rats injected only with NMDA antagonists are shown in the "controls" panel (inset). The first column on the **insert** diagram displays the number of Fos-stained nuclei following saline injection. **(B)** results of cell counts in the granule cell layer of the dentate gyrus in antagonist-pretreated and 4-AP-injected rats compared with animals injected only with 4-AP. **(C)** results of cell counts in the hippocampus and hilus of the dentate gyrus in antagonist-pretreated and 4-AP-injected rats compared with animals injected only with 4-AP. Asterisks denote significant differences ($p < 0.001$; ANOVA, *post hoc* Bonferroni-test); SEM is indicated in every case; IR, immunoreactive.

In our former studies *(Szakács et al., 2003)* the NMDA-subtype ionotropic glutamate receptor antagonists (such as amantadine, dextrometorphan, ketamine and MK-801) in pretreatment significantly decreased the expression of *c-fos* in the examined neo- and allocortical areas in the 4-aminopyridine acute convulsive rat model ***(Fig. 5)***; and in the same time, the latency of the GTCS was significantly increased (dextrometorphan, ketamine) or the GTCS occurrence was significantly reduced (MK-801) ***(Table 1)***, as well.

Compound/s	GTCS Latency (min)	SEM	Animals Displaying GTCS (%)
4-AP	30.3	1.4	100
4-AP + amantadine	26.2	2.0	100
4-AP + dextrometorphan	45.0*	4.3	83.3
4-AP + ketamine	45.3*	4.7	61.1
4-AP + MK-801	34.2	4.5	27.7▲

Table 1. Behavioural analysis of the effect of the NMDA receptor antagonism on 4-AP seizures *(Szakács et al., 2003).* The tests were conducted in groups of 15 animals each. The antagonists were injected i.p. 10 min later, 4-AP was administered, and the latencies of the onset of GTCS were measured from the time of the 4-AP injection. Significant differences are indicated. Abbreviations: GTCS, generalised tonic-clonic seizures; SEM, standard error of the mean. *$p < 0.05$; ANOVA followed by the *post hoc* Bonferroni test. Seizure occurrence: black triangle indicates the significant difference vs. control group (vehicle + 4-AP). ▲ $p<0.05$ Fisher's exact probability test.

2. OBJECTIVES

A. Based on the success of our cooperating partners in the fMRI description of the pilocarpin epilepsy paradigm *(Fabene et al., 2003)*, we proposed a pilot experiment for the fMRI study of the 4-AP acute convulsion model *(Fabene et al., 2006)* concerning the changes in the regional cerebral blood flow (rCBF) and apparent diffusion coefficient (ADC) regarding the water movements (extra- and intracellular oedema).

B. The aim of the AMPA receptor antagonism study *(Weiczner et al., 2008)* was to assess the antagonism of another well-characterised *(Alexander and Peters, 2000)* glutamate receptor, the AMPA receptor in a similar (4-AP-induced acute convulsion) paradigm. According to the time-course of the GYKI 52466 anticonvulsive efficacy *(Lees and Leong, 2001; Jakus et al., 2004)*, and based on our preliminary data we focused on the investigation of the short-term effects (*c-fos* expression and pericapillary astrocyte swelling) within the very first hour of seizure initiation. To evaluate the activation status changes of the inhibitory cells in the 4-AP paradigm, we also investigated the effect of the AMPA receptor antagonism by assessing the *c-fos* expression pattern of the immunohistochemically well-detectable parvalbumin (PV)-positive cells *(Schwaller et al., 2004)* representing a subpopulation of GABAergic interneurons *(DeFelipe, 1997)*.

C. The NMDA antagonists significantly decreased seizure-related astrocyte swelling in the cerebral cortex *(Zádor et al., 2008)*, so we are going to compare the efficacy of NMDA and AMPA receptor antagonism on the astrocyte swelling and neuronal activation (c-fos expression) associated with acute convulsions.

3. MATERIALS AND METHODS

3.1 Functional and structural MRI measurements in the 4-AP paradigm

3.1.1 Animals and treatment

The MRI experiments were performed in the Experimental MRI Laboratory of the Department of Anatomy and Histology, Faculty of Medicine, University of Verona, Verona, Italy. Male adult Wistar rats (80–90 days of age) were kept under controlled environmental parameters and veterinarian control. The animals were habituated to handling for at least 2 weeks prior to the procedures employed in the present study. The experiments received authorization from the Italian Ministry of Health and conformed to the principles of the NIH Guide for the Use and Care of Laboratory Animals and the European Community Council (86/609/EEC) directive. All efforts were made to minimize the number of animals used and avoid their suffering. Rats were randomly divided into two groups: in twelve rats, seizures were induced by 4-AP as described in previous studies *(Mihály et al., 2001)*. Seizures were elicited with a single intraperitoneal (i.p.) bolus of 4-AP (5 mg/kg 4-AP; Sigma Chemical Co., St. Louis, MO), dissolved in physiological saline (0.67 mg/ml). Control animals (n = 12) received the same volume of physiological saline i.p. MRI analysis was performed 2 h, 24 h and 3 days after seizure arrest. Twelve animals for both conditions were analysed with structural (T2W and DWI) and functional (rCBV) MRI.

3.1.2 Experimental procedure

MRI experiments were performed using a Bruker Biospec Tomograph (Bruker Medical, Ettlingen, Germany) equipped with an Oxford, 33 cm bore, horizontal magnet operating at 4.7 T and a Bruker gradient insert (maximum intensity 20 G/cm). The rats were anesthetized by inhalation of a mixture of oxygen and air (1 L/min) containing 1% of halothane (initial dose 4% halothane) 2, 24 and 72 h after seizure onset; rectal temperature and heart beat rate were monitored by Biotrig® physiological monitor (Bruker, Germany) and were similar in control and experimental animals. The rats were placed into a 7.2 cm i.d. (internal diameter) bird cage transmitter coil. The signal was received through a 2 cm surface coil, actively decoupled from the transmitter coil and placed directly on the animal's head. Three mutually perpendicular slices were acquired through the brain as scout images. Five contiguous, transversal, T2W, 2-mm-thick slices were imaged starting 1 mm posterior to the olfactory bulbs. T2W images were acquired using a RARE (rapid acquisition-rapid enhancement) sequence with the following parameters: repetition time (TR) = 5117 ms; echo time (TE) = 65 ms, RARE factor = 8; field of view

(FOV) = 4 x 4 cm^2, matrix size 256 x 256 corresponding to an in-plane resolution of 156 x 156 μm^2. In all animals, one slice was imaged using a multi-echo spin-echo sequence with 8 echoes, TR = 2000 ms and TE ranging from 25 to 200 ms for quantitative T2 mapping. The selected slice was also imaged using a diffusion-weighted spin-echo sequence, with TR = 1500 ms, TE = 60 ms, two b-values (6 and 1034 s/mm^2) and matrix size 128 x 64 zero-filled at 128 x 128. For DWI, the apparent diffusion coefficient (ADC) maps in the brain were obtained pixel by pixel by two point linear fit of the logarithm of signal intensity (M) versus the b-factors. ADC and T2 values were extracted from the relative maps using the region-of-interest (ROI) method: 5 square ROIs of 2 x 2 pixels were defined in every selected brain region for each side. In each selected brain region, the variation of ADC value between the control and experimental animals was evaluated.

As for contrast medium, Sinerem®, an USPIO *(**u**ltrasmall **s**uper**p**aramagnetic **i**ron **o**xide)* particle (kindly supplied by Guerbet, Aulnay-Sous-Bois, France), was used as contrast agent. Sinerem® is constituted by an iron-oxide core of about 6 nm diameter coated by dextran (coated particle dimensions of about 20 nm) and is characterized by a blood-half time longer than 2 h in rats *(Dousset et al., 1999)*. Sinerem® was dissolved in saline and injected at a 6 mg/kg dose (mg is referred to iron). Animals were anesthetized as indicated above, and the tail vein was catheterized for contrast medium administration. A RARE sagittal acquisition was performed in order to localize the olfactory bulb. Starting 1 mm posterior to it, 5 slices, 2-mm-thick, were acquired axially, using a RARE sequence. Three slices were chosen for regional blood volume (rCBV) mapping. After localized shimming over these slices, a gradient-echo sequence was acquired before contrast medium injection and, 2 min later. Due to the presence of air, rCBV maps could not be acquired in the brain areas located in the plane of the internal acoustic meatus, such as the amygdala and piriform cortex.

3.1.3 Analysis of the MRI data

Images were analysed using the software ParaVision® 2.1.1 (Bruker, Germany). After injection of a super-paramagnetic contrast agent, the T2* relaxation rate in the brain decreases (compared to the pre-injection baseline) proportionally to the local CBV times a certain function of the plasma concentration of the contrast agent *(Mandeville et al., 1998)*. In this work, we have normalized the rCBV values obtained in brain by the value obtained in muscle. A similar approach has been recently used *(Bremer et al., 2003)* in a study aimed at investigating blood volume in an experimental tumour model. Maps of rCBV were obtained using the algebra tool of ParaVision®. Briefly, after absolute reconstruction of images, background noise below threshold value (fixed by the ParaVision® software) was cut off, as routinely done. The natural logarithm of the ratio

between the SI before and after contrast medium administration (R value) was then calculated pixel by pixel and displayed. Values of rCBV were extracted using ROIs. Pseudocolour images were obtained using Matlab® software (Mathworks Inc.; Natick, MA). MRI data were analysed for the statistical evaluation by the mean of the software SPSS. For MRI data, difference between DWI, T2W and rCBV values obtained in control vs. 4-AP-treated rats was evaluated with one-way analysis of variance (ANOVA) for repeated measures followed by the LSD post-hoc test, setting the significance at $p < 0.05$.

3.2 Administration of the glutamate-receptor antagonists

3.2.1 Animals and treatment

The animal experiments were conducted in accordance with prevailing laws and ethical considerations (European Community Council Directive of November 24, 1986 (86/609/EEC) and the Hungarian Animal Act (1998). Written permission was obtained in advance from the Faculty Ethical Committee on Animal Experiments (University of Szeged). The animals were maintained under standard animal housing conditions, with *ad libitum* access to food and water. The experiments were performed on male Wistar rats weighting 200-250 g. The convulsant agent 4-AP (Sigma, St. Louis, MO) was dissolved in physiologic saline (0.67 mg in 1 ml vehicle) and administered intraperitoneally (i.p.), in 5 mg/kg dose. In previous investigations *(Mihály et al., 1990)*, this dosage proved to be convulsant. The non-competitive NMDA receptor antagonist MK-801 (dizocilpine maleate, Sigma, St. Louis, MO) was dissolved in physiological saline and administered i.p. in a volume of 1 ml, 10 min prior to the application of 4-AP in 1 mg/kg dose. The non-competitive AMPA receptor antagonist GYKI 52466 (IVAX GYKI Co-Ltd., Budapest, Hungary) was dissolved in 50% DMSO *(de Sarro et al., 1995)* (dimethyl-sulphoxide; Sigma, St. Louis, MO) dilution (3.33 or 6.67 mg in 1 ml vehicle), and administered i.p. 15 min before 4-AP injection, in 25 or 50mg/kg dose, respectively.

3.2.2 Experimental procedure

For the MK-801-pretreatments, the animals were randomly divided into three groups. In the first group, the animals (n=18) were pretreated with 1 mg/kg MK-801; and 10 min later, the convulsant 5 mg/kg 4-AP was administered. The control group (n=18) received the solvent of MK-801 and 5 mg/kg 4-AP. The experiments were finished 1, 3 and 24 h after the 4-AP injection (6-6-6 animals pro every time group). At the end of the experiments, three-three animals from every group were sampled for PCR *(Zádor et al., 2008)* or were processed for electron microscopy, respectively *(see below)*.

For the GYKI 52466-pretreatments, the animals were randomly divided into three groups. In the first two groups, the animals (10 per group) were pretreated with 25 mg/kg or 50 mg/kg GYKI 52466, respectively. 15 min later, the convulsant 5 mg/kg 4-AP was administered. The control group (10 animals) received the solvent of GYKI 52466 and 5 mg/kg 4-AP. The experiments were finished 1 h after the 4-AP injection, within the range of the presumed maximal anticonvulsive effect of the GYKI 52466 ***(Fig. 14).***

For the immunohistochemical evaluation of the possible individual c-fos expression effect of the applied antagonists, another four control groups have been established (N=4 in each group), as follows: animals receiving physiological saline only (1 ml for an animal with 200 g bodyweight), animals receiving 50 mg/kg GYKI 52466 only, animals receiving 1 mg/kg MK- 801 only and animals receiving 5 mg/kg 4-AP only. These animals have been sacrificed 1 h after the injection and processed for immunohistochemistry as described below.

At the end of the experiments, the animals were deeply anaesthetised with diethyl-ether and perfused transcardially with 250 ml of 0.1 M phosphate-buffered saline (PBS) pH 7.4; followed by 300 ml of fixative (four animals randomly for immunohistochemistry: 4% phosphate-buffered paraformaldehyde, pH 7.4; four animals randomly for electron microscopy: 1% paraformaldehyde and 1% glutaraldehyde in phosphate-buffered solution, pH 7.4). In case of the brains for immunohistochemistry, they were rapidly removed, postfixed in 4% paraformaldehyde for 1 h, and then cryoprotected overnight (30% sucrose in 0.1 M phosphate buffer, pH 7.4) at room temperature. Serial frozen sections were cut on a cryostat (Reichert-Jung Cryocut 1800) in the coronal plane at a thickness of 24µm and every third section was processed for immunohistochemistry ***(3.2.4)***. In case of the brains for electron microscopy, they were rapidly removed, and then we followed the routine procedure as described below ***(3.2.6)*.**

3.2.3 Analysis of the behavioural data

The behavioural outcome (effects concerning seizure activity and possible adverse effects) of the pretreatment with the AMPA antagonist was observed up to 1h after the 4-AP injection. The onset of the GTCS was always sudden and clear-cut, so the latency (from the 4-AP injection) of GTCS was easily measurable. The GTCS latency was statistically evaluated with one-way analysis of variance (ANOVA) followed by the Bonferroni *post hoc* test (significance criterion was 0.05). The GTCS occurrence and overall mortality data were analysed with the Fisher's exact probability test (significance criterion was 0.05). The statistical analysis was performed with the SPSS 9.0 software.

3.2.4 Immunohistochemistry

On the coronal brain slices *c-fos* and parvalbumin double-labelling immunohistochemistry was carried out. The sections were pretreated with Triton X-100 and H_2O_2 (9:1) solution, then they were incubated in 20% normal pig serum, avidin and biotin; then in the primary antibody cocktail with *c-fos* antibody (1:2000; raised in rabbit, Santa Cruz Biotechnology, CA) and parvalbumin (1:60000; raised in mouse, Sigma-Aldrich). The secondary antibody cocktail contained biotinylated goat-anti-rabbit (B-GAR, 1:400; Jackson ImmunoResearch, PA) and goat-anti-mouse (GAM, 1:400; Jackson ImmunoResearch, PA) antibodies. The tertiary antibodies were STA-PER (1:1000, Jackson ImmunoResearch, PA) and mouse-PAP (1:1000, Jackson ImmunoResearch, PA). The peroxidase reactions were localised with diaminobenzidine tetrahydrochlorid (Sigma-Aldrich) with nickel chloride, yielding black reaction product *(c-fos)* or without nickel chloride, yielding brown reaction product *(parvalbumin)*.

3.2.5 Analysis of the immunohistochemical data

Quantitative analysis was performed on five sections per animal (N=4; the mean data per each animal was used in the statistical analysis), selected from every brain on the basis of the same stereotaxic coordinates *(Paxinos and Watson, 1998)*. Areas of interests (AOIs) for counts of immunostained neuronal nuclei were selected form the S1Tr region of the parietal neocortex, regions CA1, CA2 and CA3 of the Ammon's horn and from the hilus and granule cell layer of the dentate gyrus. Within every AOI, the immunoreactive (IR) cells (cell nuclei for *c-fos* and cells for PV) were counted using a NIKON Eclipse 600 microscope equipped with a SPOT RT Slider digital camera (1600 x 1200 dpi in 8 bits), using the Image Pro Plus 4 morphometric software (Media Cybernetics, Silver Spring, MD). Following background subtraction, the threshold was determined so that all labelled nuclei could be recognised. The counting was performed blindly of the animal's treatment. The AOIs were determined using the rectangular field of the camera. In the neocortex, cell counts were done using a 10x objective, and the AOI (an area of 1.2 mm^2) included all neocortical layers (I-VI) from the pia mater to the subcortical white matter. Cell counts were then normalised to 1 mm^2. In the hippocampus, cell counts were done using a 40x objective, and were again normalised to 1 mm^2. In regions CA1-3, the AOI (an area of 0.05 mm^2) included the stratum pyramidale and a narrow zone of the strata oriens and radiatum. The hilus of the dentate gyrus was outlined according to Amaral *(Amaral, 1978)*, and counting was performed. The whole extent of the upper and lower blades of the dentate granule cell layer was outlined and used as AOI, and labelled cell nuclei were counted in this area. The quantitative assessment of the parvalbumin-positive cells was

omitted in the granular layer of the dentate gyrus, due to the many, strongly *c-fos* immunoreactive cell nuclei. The data were analysed statistically comparing sets of findings with the same magnification. Differences in the number of *c-fos* positive or *c-fos* and parvalbumin double-positive cells in the control and in the antagonist-pretreated were analysed with one-way analysis of variance (ANOVA), followed by the Bonferroni post hoc test. A significance criterion of 0.05 was used. The statistical analysis was performed with the SPSS 9.0 software.

3.2.6 Electron microscopy

Samples of the right parietal neocortex *(for MK-801 experiments)*; or right parietal neocortex and hippocampus *(for GYKI 52466 experiments)* were prepared for electron microscopy. The tissue blocks were incubated in an aqueous solution of 1% OsO_4 and 5% $K_2Cr_4O_7$ (1:1) after thorough rinsing. The samples were dehydrated, incubated in 1% uranyl-acetate and embedded in Durcupan epoxy resin (Fluka, Buchs, Switzerland). Semithin sections were cut on an ultramicrotome (Ultracut E, Reichert-Jung, Vienna, Austria) and stained on object glasses with a 1:1 mixture of 1% methylene blue and 1% Azure II blue. The samples were then coverslipped with DPX and analysed under a light microscope (Nikon E600, Nikon Co., Tokyo, Japan). Ultrathin sections were cut of the same blocks and collected on 200 mesh copper grids. The preparations were then contrasted with 5% uranyl-acetate and Reynolds lead-citrate solution. Finally, the samples were analysed by a Philips TM10 transmission electron microscope (Eindhoven, Netherlands). Photographs were taken with a computer assisted digital camera (MegaView II, Soft Imaging Systems, Münster, Germany).

3.2.7 Analysis of the electron microscopical data

Approximately 900 μm^2 of sample surface was viewed systematically through all neocortical layers of the parietal cortex or in the hippocampus; 4 EM preparates per animal (N=4) was examined and the mean data of the altogether 14 ± 2 capillary cross sections per each animal was used in the statistical analysis. The total area of the so-called neurovascular unit was measured which consists of the capillary lumen, the surrounding endothelium and the astrocytic end-feet covering the basal lamina of the microvascular endothelium. (Image Pro Plus 4.5 morphometric software; Media Cybernetics, Silver Spring, MD, USA). One-way analysis of variance (ANOVA) followed by the Bonferroni *post hoc* test, (significance criterion: $p<0.05$; SPSS 9.0 statistical software) was performed on the measured area data (area of capillaries, area of the swollen pericapillary astrocytic endfeet).

4. RESULTS

4.1 Structural MRI of the 4-AP model

4.1.1 T2 maps

Quantitative T2 maps calculated from multi-echo spin-echo acquisitions ***(Fig. 6 E–H)*** clearly showed the overall pattern of changes in control and epileptic rats (both at 2 h and 24 h), highlighting the signal increase throughout the cerebral cortex. The T2 value was also slightly increased in the amygdala. In the diencephalon, selective increase in the T2 signal was documented in medial thalamic regions. T2 values exhibited a 56% increase ($p<0.001$) in the parietal cortex at 2 h vs. control; this increase was still present ($p<0.01$) at 24 h (+29%). A dramatic increase in the T2 values was found also in the hippocampus after 2 h (+72%, $p<0.001$) and after 24 h (25%; $p<0.01$). The temporal cortex showed the same pattern of alteration (+97%; $p<0.0001$ at 2 h; + 39%, $p<0.001$ at 24 h). A highly significant ($p<0.001$) increase in T2 (52% at 2 h and 33% at 24 h) was also found in the medial thalamus. In all of these structures, the T2 values observed 24 h after seizures were significantly higher than those observed in the controls ($p<0.001$). No evident differences were detected 3 days after seizure induction ***(Fig. 6 H, N)***.

4.1.2 Diffusion-weighted imaging

Diffusion-weighted images, based on the sensitization of the MRI signal to the Brownian motion of water molecules, reveal maps of brain tissue water motion, resulting in hyperintense alterations. ADC maps of brain tissue water, calculated from DWI, showed consistent changes in ADC in the cerebral cortex (parietal cortex), hippocampus and amygdala of the epileptic animals at 2 h and 24 h ***(Fig. 6 B–C)*** compared with control ones ***(Fig. 6 A)***. An evident reduction of the average ADC value was documented in the parietal (-44%) and temporal (-34%) cortices, hippocampus (-23%) and medial thalamus (-11%) 2 h after 4-AP-induced seizures ***(Fig. 6 B, M)***. A further drop of ADC value was documented 24 h after 4-AP injections in the hippocampus (-46%), medial thalamus (-21%) and in the cerebral cortex (parietal: -57%; temporal: -64%) ***(Fig. 6 C, M)***. ADC values returned to basal levels 3 days after seizure onset ***(Fig. 6 D, M)***.

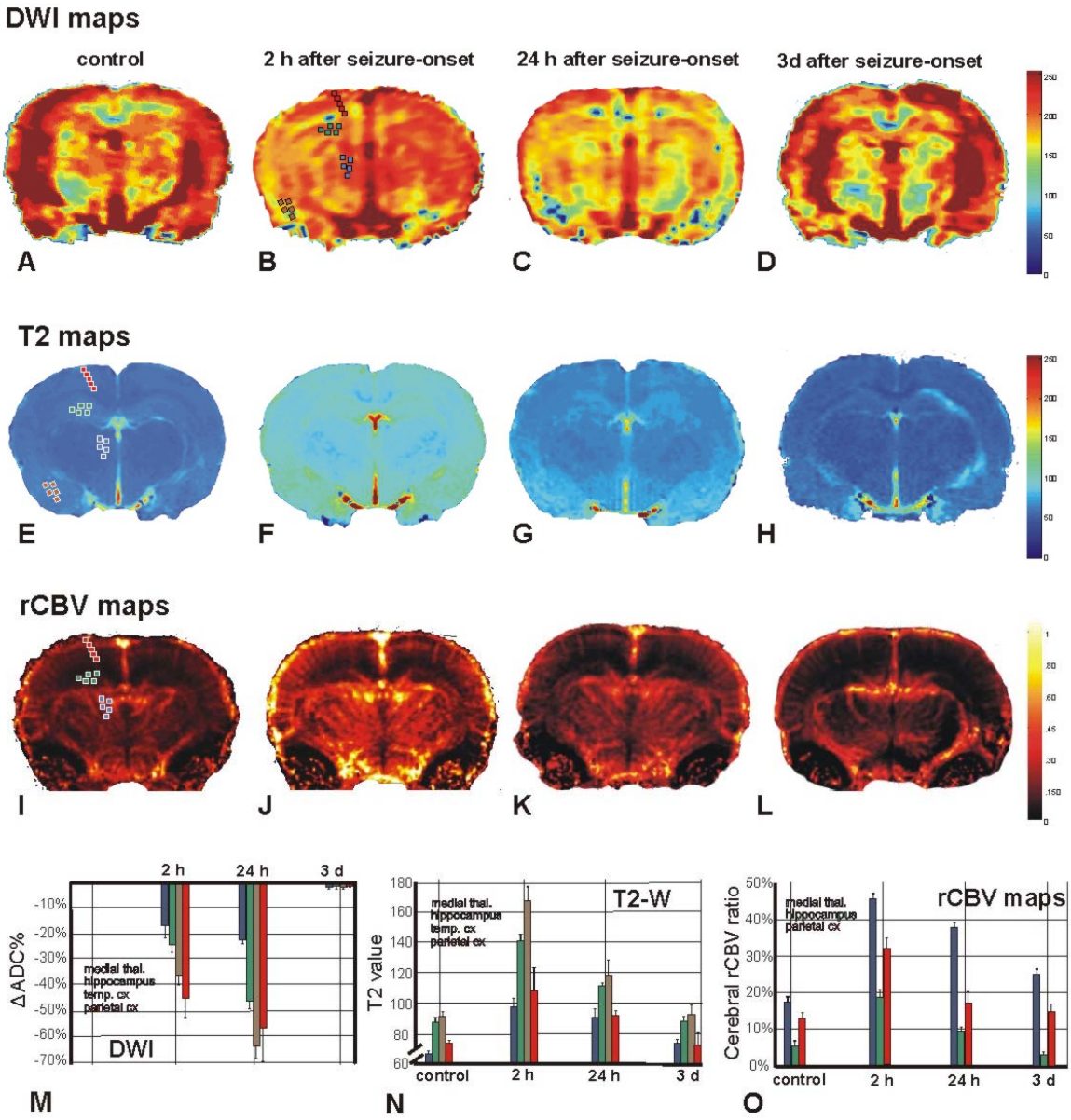

Fig. 6: Parametric maps showing diffusion-weighted images in control (A) and experimental (2 h, 24 h and 3 days after seizures, **B– D**, respectively) **conditions.** T2 parametric maps are represented in **E** (control), **F** (2 h), **G** (24 h) and **H** (3 days after seizure onset). Regional cerebral blood volume maps are shown in the three different experimental conditions (**I** = control, **J** = 2 h, **K** = 24 h and L = 3 days after seizure). **(M–O)** Graphic representations of the above mentioned parameters in different brain structures. Boxes in **B, E, I** represent the different ROIs used in the data analysis; squares are drawn only in one side, while the data acquisition was performed on both sides. Blue bars represent the medial thalamus, green bars represent the hippocampus, brown bars represent temporal cortex, while red bars represent parietal cortex in panels **M–O**.

4.2 Functional MRI of the 4-AP model: *rCBV maps*

Quantitative parametric maps reconstructed by images acquired with gradient-echo sequence before and after USPIO administration in control and epileptic animals at 2 h and 24 h ***(Fig. 6 I–K)*** showed an increase of average blood volume value in the early stages of the seizures, with a progressive normalization of the values at 24 h ***(Fig. 6 K)*** in

the parietal cortex and hippocampus. In the medial thalamus, the value failed to return to baseline 24 h post-convulsions ($p<0.001$). 2 h after seizure onset, the values were higher in the parietal cortex (+32%, $p<0.0001$) and in the hippocampus (+16%, $p<0.01$) versus control. At subcortical levels, rCBV increased in the medial thalamus (+44%, $p<0.0001$). 24 h after seizures, rCBV showed marginal alteration in the parietal cortex (+4%) and hippocampus (+4%) but was still highly significantly ($p<0.0001$) increased (+21%) in the medial thalamus. No significant alterations were found 3 days after seizure onset ***(Fig. 6 L, O)***.

4.3 Behavioural analysis of the pretreatments with GYKI 52466

The i.p. administration of 4-AP causes characteristic behavioural symptoms ***(Fig.7 A-F)*** within 15-20 min *(Mihály et al., 1990)*: increased exploratory activity, tremor of the vibrissal and masticatory muscles, followed by generalised tremor of the body musculature, observable as continuous fasciculation of the muscles, the more and more frequent clonuses and tonus changes of the limbs. Abduction of the posterior limbs and a fan-like abduction of the fingers are also observable. The increasing motor symptoms lead to a "wild running" phenomenon and, finally, to generalised tonic-clonic seizures (GTCS), often preceded by vocalisation.

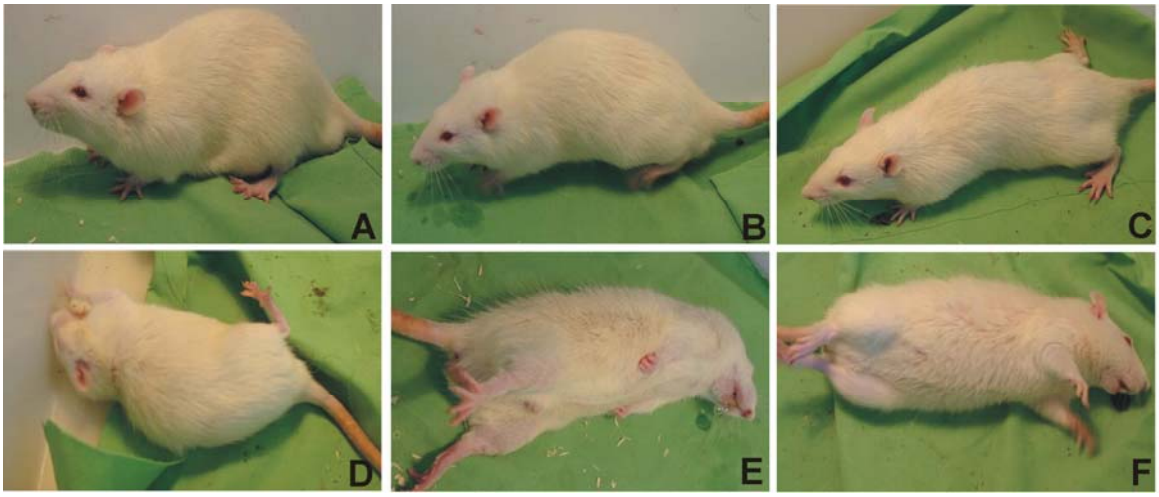

Fig. 7: The characteristic symptomatic appearance of the 4-AP-induced acute seizure activity. Early symptoms: increased exploring activity, tremor of vibrissal and masticatory muscles **(A)**, sniffing, washing behaviour. The generalised tremor, the continuous fasciculation of muscles, the frequent clonic movements of limbs can be noticed **(B)**. The muscle tone changes, the abducted position of hind limbs and the fan-like abduction of toes are also characteristic **(C)**. The increasing motor symptoms finally result in GTCS **(D)**, sometimes introduced by wild running or vocalisation. During GTCS, the limbs are in extension, hypersalivation and the release of excreta are also common signs **(E)**. After the solution of the tonic phase, the seizure activity is rather clonic, with simultaneous tenebrosity of the animal for 10-15 min **(F)**. Repeated GTCS is can be frequently noticed. After 50-60 min, the seizure activity gradually decreases, most of the animals regenerate after 90 min (counted form the 4-AP injection). Nevertheless, in some cases GTCS can lead to the death of the animal. *(Photographs: Department of Anatomy, Szeged).*

The limbs are extended; hypersalivation and release of excreta are regular. With the dissipation of the tonic component, the clonic one becomes more dominant for a while with tenebrosity (post-convulsive state with limited cognitive and motor activity) for other 10-15 min until regaining normal activity. In some cases the GTCS may occur once more. The gradual dissipation of the seizure activity can be detected electrophysiologically after 50-60 min *(Mihály et al., 2005)*; 90-100 min after the 4-AP injection, the animals recover. Nevertheless, approximately 20% percent of the control group animals die during or after GTCS, due to the seizure. The onset of the GTCS was always sudden and clear-cut, so the latency (from the 4-AP injection) of GTCS was easily measurable.

The increase in the GTCS latencies of the GYKI 52466-pretreated groups is observable but statistically do not differ between the two dose groups, however, they represent a significant change compared with the control group ***(Table 2)***. In the pretreated groups, the GTCS occurred in 20% (25 mg/kg) or in 10% (50 mg/kg) of the animals, whilst in 80% of the 4-AP control animals (without GYKI 52466 pretreatment). According to the Fisher's exact probability test, reduction in the number of animals (in which a GTCS occurred) in both groups administered GYKI was statistically significantly different from the number in the vehicle treated group. Nevertheless, there is no significant difference between the groups with different GYKI 52466 doses. During the 1-hour observation, no recurrent GTCS was observed, the survival ratio was 100% in both pretreated groups, whilst 80% in the control group; which is, however, statistically not significant.

Pretreatment	Treatment	mean GTCS latency (min)	SEM	Animals displaying GTCS (%)	Mortality (%)
vehicle of GYKI 52466 i.p.	5 mg/bwkg 4-AP i.p.	26.60	1.81	80	20
25 mg/bwkg GYKI 52466 i.p.	5 mg/bwkg 4-AP i.p.	49.57*	2.31	20▲	0
50 mg/bwkg GYKI 52466 i.p.	5 mg/bwkg 4-AP i.p.	46.75*	4.21	10▲	0

Table 2. Behavioural analysis of the effect of the AMPA receptor antagonism on 4-AP seizures *(Weiczner et al., 2008)*. The observation was made with 10 animals in each group. The GTCS (i.e. generalised tonic-clonic seizure) latency was measured from the administration time of the 4-AP injection. Mean GTCS latency: asterisk indicates the significant difference vs. control group (vehicle + 4-AP). * $p<0.05$ ANOVA followed by the Bonferroni *post hoc* test. Seizure occurrence and mortality: black triangle indicates the significant difference vs. control group (vehicle + 4-AP). ▲ $p<0.05$ Fisher's exact probability test.

Besides the local –presumably peritoneal– irritation (at the site of injection) dissipating within 1-2 min after the DMSO administration (as vehicle in the control group), no long-lasting side-effect of DMSO was noted, the animals displayed normal activity. As observable side-effects of the GYKI 52466 pretreatment, transient (approximately 15-20 min before regaining normal activity) ataxia, loss of coordination and reduction of the

locomotor activity, together with apparently sedative effect (decreased vigilance) were noted (i.e. the animals stopped the explorative movements, laid down at the floor of the cage, breathing evenly similar to sleeping, their overall muscle tone appeared to be reduced at holding or palpating the animals). These changes were pure visual observations; no methodical evaluation was performed on these parameters.

4.4 Immunohistochemistry of the pretreatments with GYKI 52466

The lower dose GYKI 52466 pretreatment (25 mg/kg) significantly increased, whereas the higher dose pretreatment (50 mg/kg) significantly decreased the number of *c-fos*-IR cell nuclei in the neocortex ***(Fig. 8)***. In laminar distribution, the laminae II-III and V-VI showed this significant decrease with the higher dose (the decrease in the lamina IV was not significant).

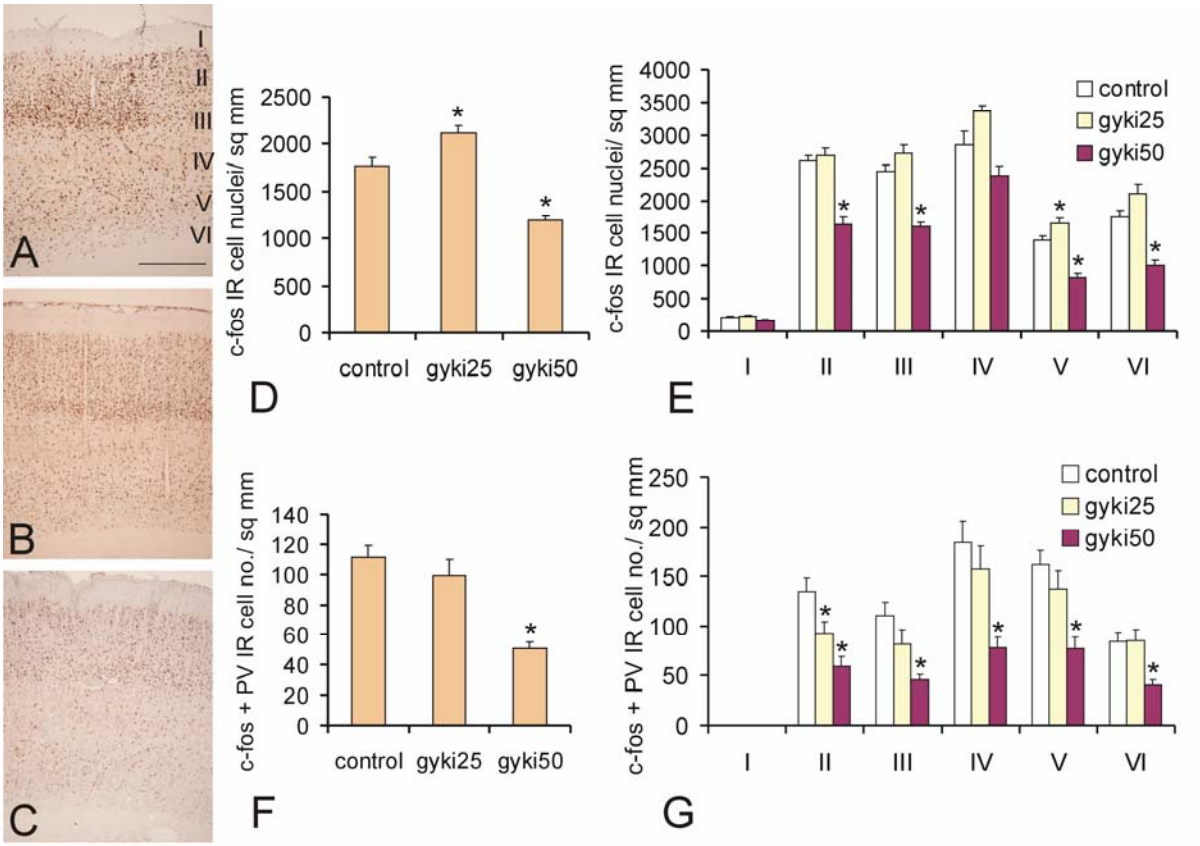

Fig. 8: Effect of GYKI 52466 on the c-fos gene expression in the neocortex *(Weiczner et al., 2008)*. **A-C.** Representative immunohistochemical images illustrating the c-fos and c-fos + parvalbumin (PV) immunolabelled neurons in the neocortex of the experimental animals. Animals with vehicle + 5 mg/ kg 4-AP (control) **(A)**; 25 mg/ kg GYKI 52466 + 5 mg/ kg 4-AP (gyki25) **(B)** and 50 mg/ kg GYKI 52466 + 5 mg/ kg 4-AP (gyki50) **(C)** treatment, respectively (N= 4 per group). Roman numerals indicate the neocortical laminae. Bar: 250 µm. Magnification: 40x. **D-G.** Statistical evaluation of the c-fos (D-E) and c-fos and parvalbumin **(F-G)** immunoreactive cell counts pro square millimetre (sq mm), in all layers **(D, F)** and in laminar distribution **(E, G)**; comparison of the data from pretreated (with 25 or 50 mg/ kg GYKI 52466 before 5 mg/kg 4-AP, respectively) and the control animals (vehicle + 5 mg/ kg 4-AP), 1h after the seizure induction. Asterisks denote the significant differences (with vs. without GYKI 52466 pretreatment); (ANOVA, Bonferroni *post hoc* test, $p<0.05$; SEM is indicated in every case).

The lower dose pretreatment yielded significant increase in the lamina V only, the other changes are statistically not significant. In the lamina I, no change was detectable in both cases. As for the *c-fos* and PV double-positive cells, the lower dose pretreatment had no effect while the higher dose pretreatment caused a significant decrease in the double-immunoreactive cell counts. This change was significant only in the lamina II for the lower dose, whereas in the laminae II-VI for the higher dose pretreatment.

In the hippocampal sectors CA1-3 and in the hilus of the dentate gyrus even the lower dose GYKI 52466 pretreatment caused significant reduction not only in the number of the *c-fos*-IR cell nuclei; but also in the number of the double-labelled cells ***(Fig. 9)***.

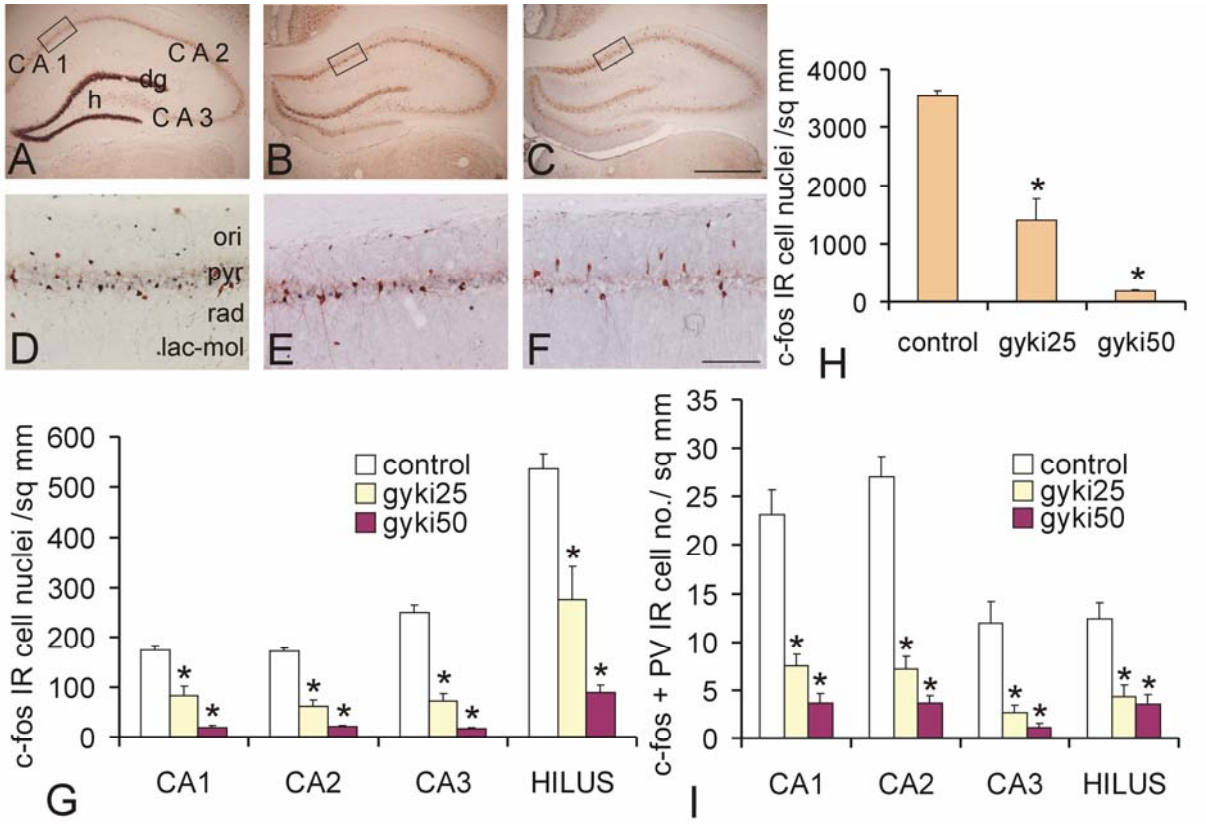

Fig. 9: Effect of GYKI 52466 on the c-fos gene expression in the hippocampus *(Weiczner et al., 2008)*. **A-F.** Representative immunohistochemical images illustrating the c-fos and c-fos + parvalbumin (PV) immunolabelled neurons in the hippocampus and dentate gyrus of the experimental animals. Animals with vehicle + 5 mg/ kg 4-AP (control) **(A, D)**; 25 mg/ kg GYKI 52466 + 5 mg/ kg 4-AP (gyki25) **(B, E)** and 50 mg/ kg GYKI 52466 + 5 mg/ kg 4-AP (gyki50) **(C, F)** treatment, respectively (N= 4 per group). Abbreviations indicate the sectors of the Ammon's horn (CA1-3); the dentate gyrus (dg); the hilus of the dentate gyrus (h); and the histological layers of the hippocampus: stratum oriens (ori), stratum pyramidale (pyr), stratum radiatum (rad), stratum lacunosum-moleculare (lac-mol); respectively. Rectangular fields note the position of higher magnification samplings. Bar: 250 µm **(A-C)**; 50 µm **(D-F)**. Magnification: 40x **(A-C)**; 200x **(D-F)**. **G-I.** Statistical evaluation of the c-fos **(G, H)** and c-fos and parvalbumin **(I)** immunoreactive cell counts pro square millimetre (sq mm), in the pyramidal layers of the hippocampal areas and in the hilus of the dentate gyrus **(G, I)** and in the granular layer of the dentate gyrus **(H)**; comparison of the data from pretreated (with 25 or 50 mg/ kg GYKI 52466 before 5 mg/kg 4-AP, respectively) and the control animals (vehicle + 5 mg/ kg 4-AP), 1h after the seizure induction. Asterisks denote the significant differences (with vs. without GYKI 52466 pretreatment); (ANOVA, Bonferroni *post hoc* test, $p<0.05$; SEM is indicated in every case).

This *c-fos*-IR count change is even more pronounced in the granular layer of the dentate gyrus ***(Fig. 9 H)***: control *c-fos*-IR nuclei (3535 per mm^2; 100%) vs. GYKI 52466-pretreatment with 25 mg/kg (1401 per mm^2; 39.6% of the control) or with 50 mg/kg (184 per mm^2; 5.2% of the control).

To assess the possible individual effects of the applied glutamate-receptor antagonists on the seizure-related c-fos induction, the c-fos IR cell counts of the control animals have been statistically evaluated. The control groups (receiving physiological saline only or 50 mg/kg GYKI 52466 only or 1 mg/kg MK-801 only; without seizure induction with 4-AP) show no significant difference compared to one another, so the effect of antagonists given alone does not differ statistically from that of the physiological saline in this acute convulsion paradigm ***(Fig. 10)***.

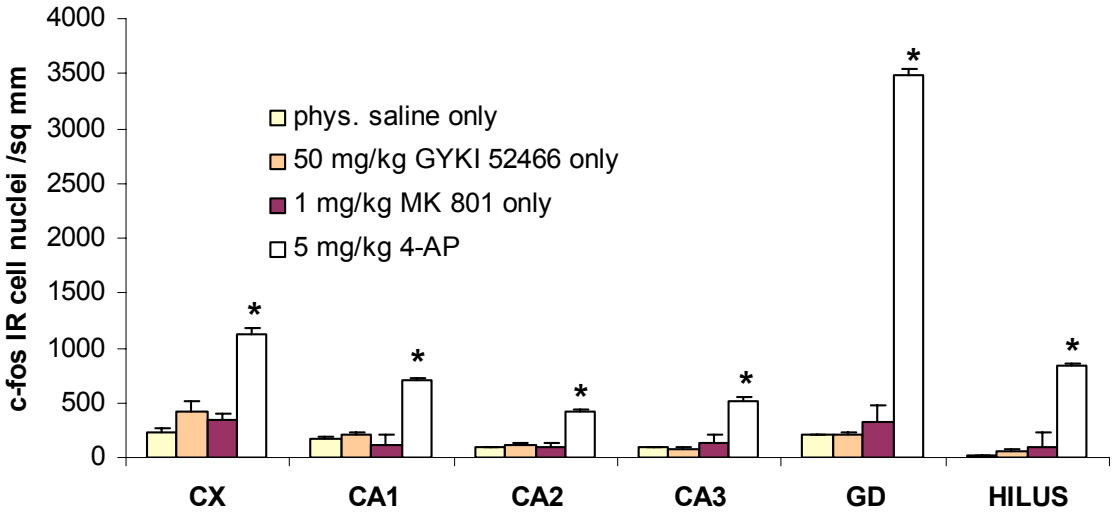

Fig. 10: Effect of MK-801 and GYKI 52466 on the c-fos IR cell counts when given alone without 4-AP. Statistical evaluation of the c-fos immunoreactive cell counts pro square millimetre (sq mm), in the parietal neocortex **(CX)** pyramidal layers of the hippocampal areas **(CA1-3)** and in the granular layer **(GD)** and in the hilus **(H)** of the dentate gyrus; comparison of the data from animals received physiological saline only or 50 mg/kg GYKI 52466 only or 1 mg/kg MK-801 only without seizure induction and animals with 5 mg/kg 4-AP, respectively, 1h after the seizure induction (N=4 per group). Asterisks denote the significant differences (animals with and without seizure induction); (ANOVA, Bonferroni *post hoc* test, $p<0.05$; SEM is indicated in every case). *Note:* the effect of GYKI 52466 or MK-801 (when given alone) on the seizure-related c-fos expression does not differ from that of the physiological saline.

4.5 Electron microscopy of the pretreatments with MK-801 or GYKI 52466

The swelling of pericapillary astrocytic endfeet (i.e. the increase of the area occupied by astrocytic glia limitans) was significantly reduced in the groups with *MK-801-pretreatment* compared to the 4-AP controls at any observed time point ***(Fig. 11)***. Regarding the capillary areas, there was no significant difference between the animal groups with and without MK- 801-pretreatment at 1h and after 24h. The only significant change at 3h

indicates that the MK-801-pretreatment significantly reduced the capillary lumen compression due to pericapillary oedema. This difference is also significant between the 1h and 3h pretreated groups.

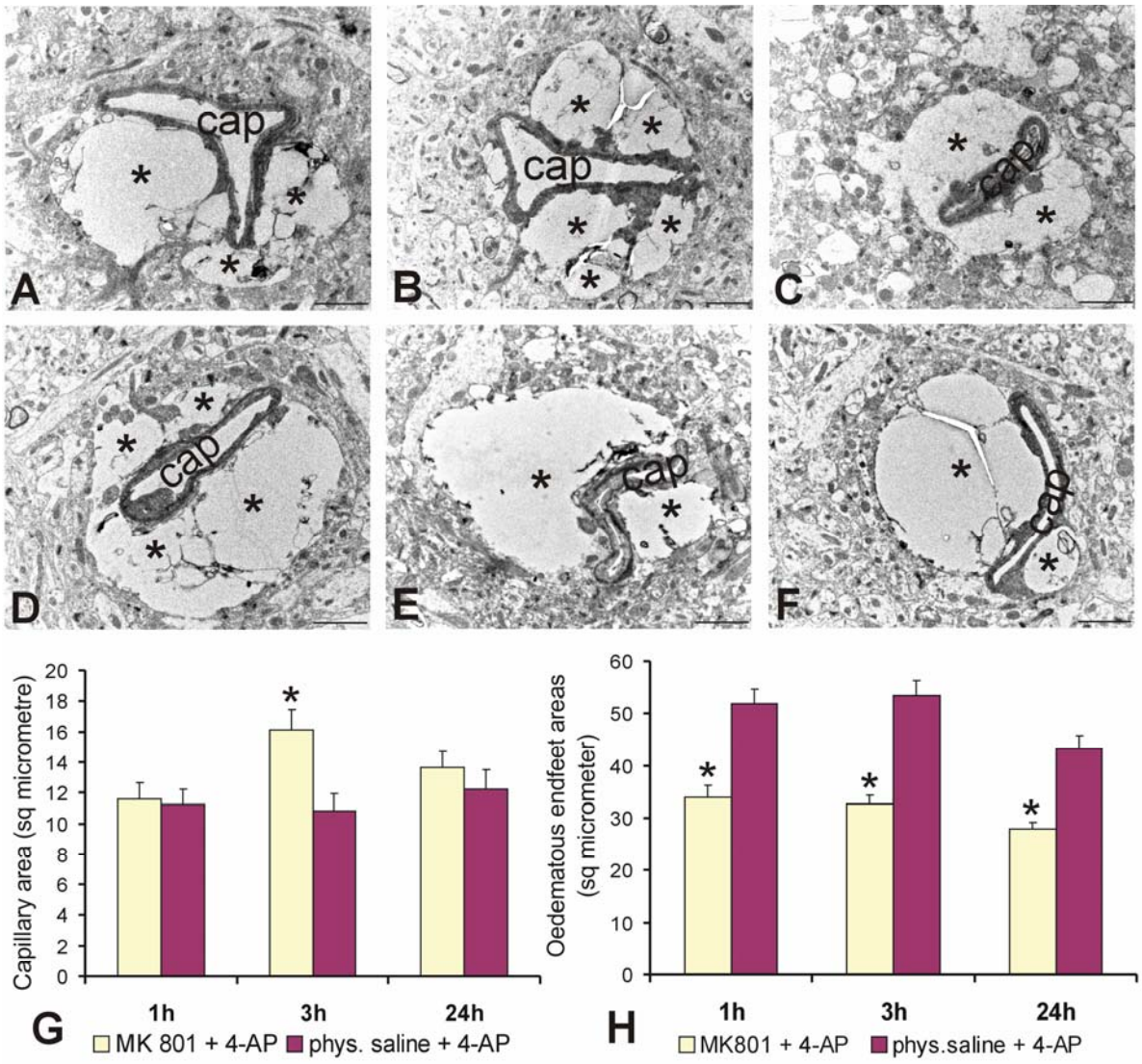

Fig. 11. Representative electron microscopic images illustrating the pericapillary astrocytic endfeet swelling in the parietal neocortices of the experimental animals. A-C. Animals with MK-801-pretreatment and 4-AP treatment: 1, 3 or 24 h after the seizure induction, respectively. **D-F.** Control animals treated with the vehicle of MK-801 (physiologic saline) and 4-AP; 1, 3 or 24 h after the seizure induction, respectively. "**cap**" indicate the capillaries; asterisks denote the surrounding oedematous astrocytic endfeet. Bar: 2 μm. Magnification: 5800x. Statistical evaluation of the capillary areas (μm^2) **(G)** and swollen pericapillary astrocytic endfeet areas (μm^2) **(H)**, comparison of the data from the MK-801-pretreated and the control animals, 1h, 3h and 24h after the seizure induction, respectively. Asterisks denote the significant differences (MK-801+4-AP vs. vehicle+ 4-AP) within the certain time groups; (ANOVA, Bonferroni *post hoc* test, $p<0.05$; SEM is indicated in every case).

In the case of the *neocortical capillary areas* ***(Fig. 12)***, there was no significant difference amongst the 4-AP control and the *GYKI 52466-pretreated* groups. The swelling of pericapillary astrocytic endfeet in the neocortex was significantly increased in the group with lower dose of GYKI 52466-pretreatment compared to the vehicle + 4-AP controls, whereas there was no significant difference between the control and the 50 mg/kg GYKI 52466-pretreated groups ***(Fig. 12)***.

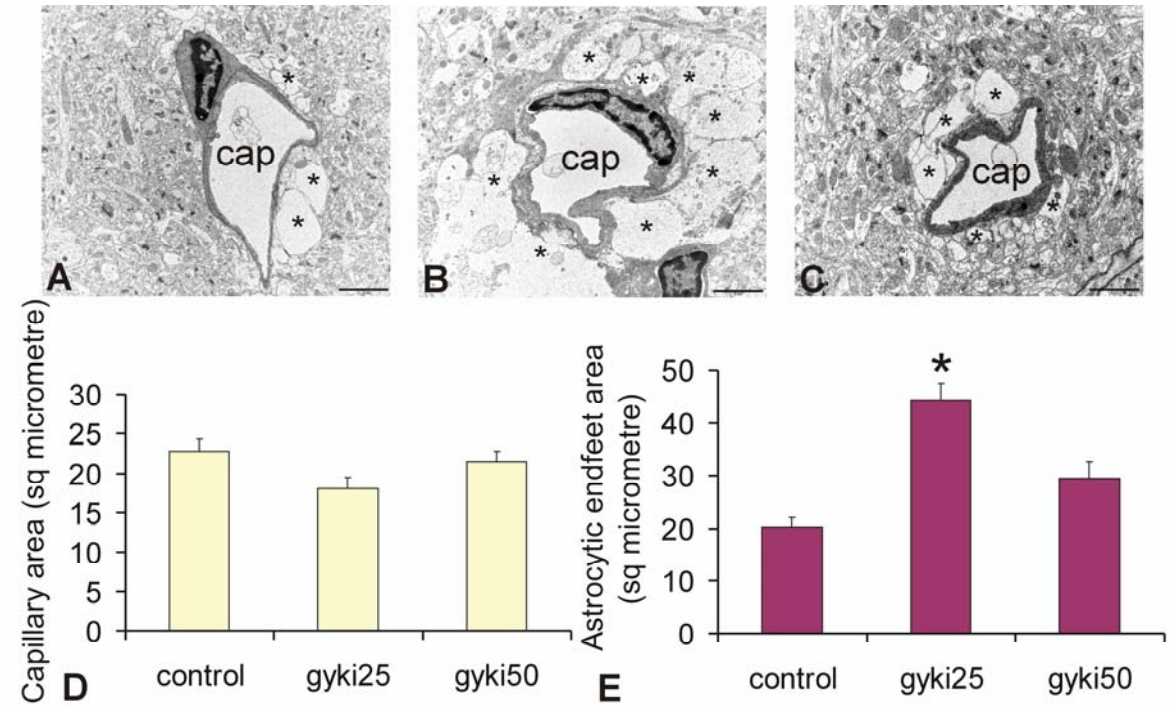

Fig. 12: Effect of GYKI 52466 on the capillary area changes and the pericapillary astrocytic process swelling in the neocortex *(Weiczner et al., 2008)*. **A-C.** Representative electron microscopic images illustrating the pericapillary astrocytic endfeet swelling in the neocortex of the experimental animals. Animals with vehicle + 5 mg/ kg 4-AP **(A)**; 25 mg/ kg GYKI 52466 + 5 mg/ kg 4-AP **(B)** and 50 mg/ kg GYKI 52466 + 5 mg/ kg 4-AP **(C)** treatment, respectively (N= 4 per group). Capillaries (cap); asterisks denote the surrounding oedematous astrocytic endfeet. Bar: 2 µm. Magnification: 5800x. **D.** Statistical evaluation of the capillary areas in square (sq) micrometre, comparison of the data from pretreated (25 or 50 mg/ kg GYKI 52466) and the control animals (vehicle + 5 mg/ kg 4-AP), 1h after the seizure induction. **E.** Statistical evaluation of the pericapillary astrocytic endfeet areas in square (sq) micrometre, comparison of the data from pretreated (25 or 50 mg/ kg GYKI 52466) and the control animals (vehicle + 5 mg/ kg 4-AP), 1h after the seizure induction. Asterisks denote the significant differences (with vs. without GYKI 52466 pretreatment); (ANOVA, Bonferroni *post hoc* test, $p<0.05$; SEM is indicated in every case).

Measuring the *hippocampal capillary areas* ***(Fig. 13)***, there was a significant difference between the 25 mg/kg GYKI 52466-pretreated and the 4-AP control group (significant decrease in the group that received the AMPA antagonist), whereas there was no such difference between the higher dose pretreatment and the 4-AP control group. In the hippocampus ***(Fig. 13)***, no significant alteration can be detected between the three groups.

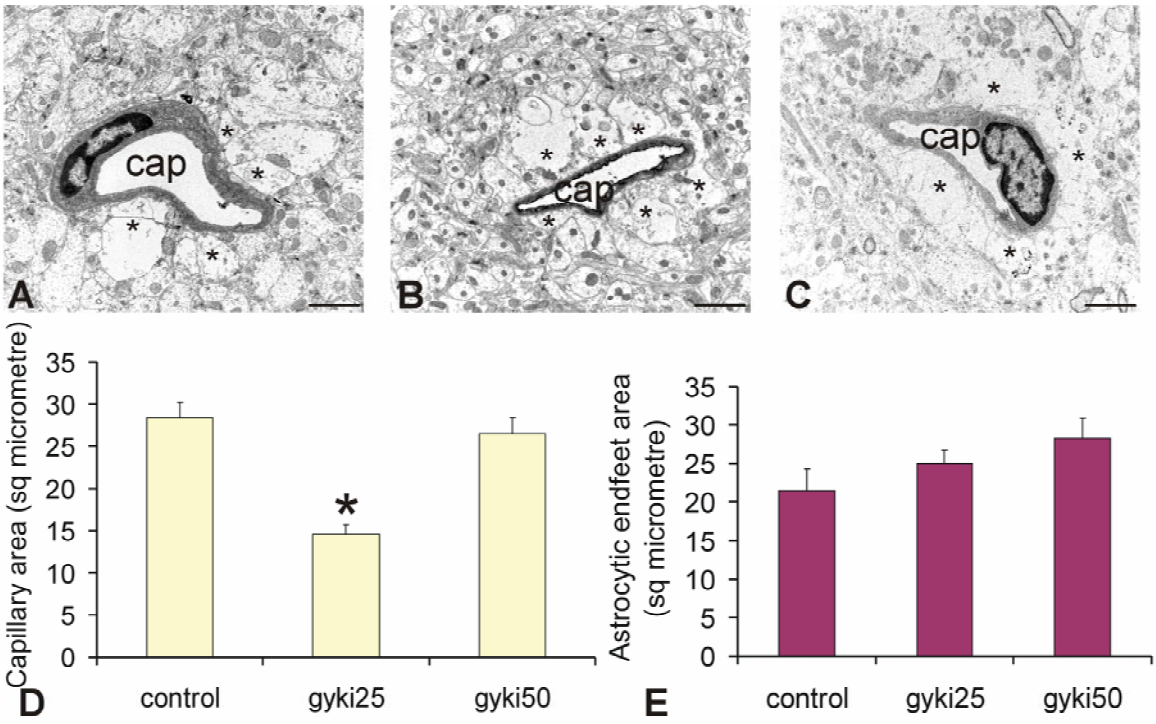

Fig. 13: Effect of GYKI 52466 on the capillary area changes and the pericapillary astrocytic process swelling in the hippocampus *(Weiczner et al., 2008)***. A-C.** Representative electron microscopic images illustrating the pericapillary astrocytic endfeet swelling in the hippocampal areas of the experimental animals. Animals with vehicle + 5 mg/ kg 4-AP **(A)**; 25 mg/ kg GYKI 52466 + 5 mg/ kg 4-AP **(B)** and 50 mg/ kg GYKI 52466 + 5 mg/ kg 4-AP **(C)** treatment, respectively (N= 4 per group). Capillaries (cap); asterisks denote the surrounding oedematous astrocytic endfeet. Bar: 2 µm. Magnification: 5800x. **D.** Statistical evaluation of the capillary areas in square (sq) micrometre, comparison of the data from pretreated (25 or 50 mg/ kg GYKI 52466) and the control animals (vehicle + 5 mg/ kg 4-AP), 1h after the seizure induction. **E.** Statistical evaluation of the pericapillary astrocytic endfeet areas in square (sq) micrometre, comparison of the data from pretreated (25 or 50 mg/ kg GYKI 52466) and the control animals (vehicle + 5 mg/ kg 4-AP), 1h after the seizure induction. Asterisks denote the significant differences (with vs. without GYKI 52466 pretreatment); (ANOVA, Bonferroni *post hoc* test, $p<0.05$; SEM is indicated in every case).

5. DISCUSSION

5.1 Functional and structural MRI in the 4-AP acute convulsion paradigm

In the present study, 4-AP-induced seizures were investigated by structural and functional MRI. Functional alterations, detected by rCBV images, were correlated to structural alterations investigated with MRI. Structural alterations were studied by T2W RARE images that were already reported to be sensitive in detecting epileptic alterations *(Fabene et al., 2003)*. T2W maps indicate that the peak of T2 alterations occurs 2 h after seizures, whereas 24 h after seizures, these values are decreased close to baseline levels. The long-lasting modification of these values has been reported after SE in animals that subsequently become epileptic, such as kainic acid and pilocarpine seizures *(Hasegawa et al., 2003; Fabene et al., 2003)*. In these chronic epilepsy models, the alterations of the T2W maps are more evident at 24 h after seizures, compared to our present findings in the 4-AP model. This fast recovery in T2W images would be consistent with the absence of an epileptogenic phase and reflected a reduced severity of the oedema following brief, acute seizures. The ADC alterations reflect pathological conditions in brain tissue that are only partially understood and involve changes in the diffusion characteristics of intra- and extracellular water compartments, water exchange across permeable boundaries *(Grass et al., 2001)* and changes in volume transmission *(Syková, 2004)*. In general, reduction of the ADC has been associated with acute cytotoxic oedema *(Fabene et al., 2003)*. Previous studies on sustained experimental seizures induced by pilocarpine *(Wall et al., 2000)*, bicuculline *(Zhong et al., 1993)*, systemic administration *(Nakasu et al., 1995; Wang et al., 1996)* or intrahippocampal injection of kainic acid *(Tokumitsu et al., 1997)* reported similar changes in ADC values in various brain areas, especially in limbic structures, and DWI was reported to provide sensitive indications on acute alterations in these paradigms *(Nakasu et al., 1995; Wang et al., 1996; Wall et al., 2000)*. The present findings of decreased ADC values in the cerebral cortex can be explained with cytotoxic oedema *(Lassmann et al., 1984)*. The swelling of the astrocytes, and the oedema of the perivascular glia limitans, suggest the presence of excess amounts of excitatory transmitters (glutamate see *Kovács et al., 2003*), metabolites (CO_2) and K^+ in the extracellular space. On the basis of the morphological results, we conclude that the brief, acute seizures caused cellular oedema of the astrocytes mainly *(Kimelberg, 2004)*. The swelling of the astrocyte obliterated brain extracellular spaces; inhibiting the clearance of transmitters, ions and HCO_3^- from the extracellular space, contributing to and enhancing the cellular damage *(Van Gelder, 1983)*. However, the astrocyte that has taken up glutamate from the extracellular space

may release it again through connexon-hemichannels *(Simard and Nedergaard, 2004)*. Therefore, the astrocyte may sustain a long-lasting decrease in volume transmission *(Syková, 2004)*. These changes may explain the long-lasting decrease of the ADC values in our experiments. We measured the prolonged decrease of the capillary lumen diameter, which may well contribute to these changes: the decrease of the capillary diameter impairs the local microcirculation *(Farkas et al., 2003)* and could contribute to the decrease of ADC values. The partial mismatch between the altered DWI values and the minor astrocytic swelling detected by histological analysis at 24 h may be partially explained by a dehydration process that affects the oedema evaluation, allowing only the detection of the more obvious alterations. The increase of rCBV at the same time may reflect the compensatory effects of the local changes at the level of the arterioles and larger vessels *(Farkas et al., 2003)*. In order to better understand CBV data, it should be considered that oedema results in the decrease of the diameter of microvessels in the affected regions, thus inducing a relative ischaemia *(Lassmann et al., 1984)*, and a compensatory hyperperfusion in adjacent areas may be hypothesized. The decrease of the luminal diameter of neocortical capillaries was measured and demonstrated in our experiments. Taken together, our data show that brain damage following SE involves several presumably pathological processes operant in both limbic and extra-limbic regions, suggesting that sustained seizure activity elicits a complex rearrangement of cortical and subcortical neural networks. The ultrastructural changes indicate different processes controlling diffusion properties of the extracellular spaces. That is, tissue layers containing neuronal cell bodies display decreased extracellular space which is apparently neurotoxic. Conversely, neuropil regions rich in synapses, small dendrites and astrocytic processes have an apparently greater capacity for the clearance of the extracellular space, which may contribute to the maintenance of the seizure process. The present study demonstrates that different MRI strategies can sensitively detect seizure-induced changes in vivo at high resolution.

5.2 Effect of the pretreatment with glutamate-receptor antagonists on the seizure-associated symptoms and seizure outcome

According to our former results ***(Table 1)***, the non-competitive NMDA receptor antagonists ***MK-801*** (given in pretreatment) significantly reduced the number of animals displaying GTCS without prolonging the seizure-latency. After the intraperitoneal administration of MK-801 the first characteristic symptoms (at the same time, these signs indicate that the drug successfully reached the central nervous system) muscle hypotonia and unsteady gait, slight impairment of postural control with stereotypic, repeated movements of the

head; due to the psychotomimetic (phencyclidine-like) side effects of MK- 801 *(Eyjolfsson et al., 2006)* developed, followed by mild tremor. The animals treated with MK-801 rarely developed generalized tonic-clonic convulsions *(Szakács et al., 2003)*; muscle tremor being the main symptom throughout the experiment.

The electrophysiological effects of ***GYKI 52466*** are well-known *(Arai, 2001)*, therefore in the present study we focused on the short-term behavioural outcomes, changes in gene expression and ultrastructural pathology, in order to asses the efficacy of the non-competitive AMPA receptor antagonist in chemically induced convulsions. The GYKI 52466 increased the latency of the first GTCS (however, without dose-dependent difference); no GTCS recurrence was observed (if there was GTCS event; only one GTCS per animal was registered during the observation). The seizure survival of the pretreated animals was 100%, however, in this case there is no significant change compared to the survival of the control group animals (80%). As for side-effects of the AMPA antagonist pretreatment, decrease in the locomotor activity *(Jakus et al., 2004)* and muscle tone were observed, likely due to the formerly described central muscle relaxant effect *(Tarnawa et al., 1989)*. Probably, this property can be responsible for the visible reduction of the tonic seizure component, and the dominance of the clonic component in the GTCS of the pretreated animals. Moreover, GYKI 52466 was found to be effective in different models of epilepsy only in doses impairing motor function *(Kubová et al., 1997)*. However, there is a controversy about whether the GYKI 52466 lacks *(Tarnawa et al., 1992; Donevan and Rogawski, 1993)* or at least partially has *(Block and Schwarz, 1994; Kubová et al., 1997)* the effects of the “conventional” 1,4-benzodiazepines (suspected in the pharmacological background of the side-effects). Nevertheless, the possibility that DMSO (as vehicle, see later), eventually potentiates not only the efficacy, but also the side-effects of GYKI 52466 cannot be entirely excluded. According to literature data, higher doses are needed for the moderation of the clonic components, than for the tonic components *(de Sarro et al., 1998)*.

After the intraperitoneal administration of GYKI 52466, the peak of blood plasma level is reached between 15 and 45 min, then, with a mostly linear pharmacokinetic fashion ***(Fig. 14)***, 100-120 min after the administration, the concentration gradually decreases to a near-zero level. Parallel with this change, the visible anticonvulsive activity of the drug is maximal between 15 and 60 min after the injection. This period can be characterised with lower seizure scores *(de Sarro et al., 1998)*, and this is why we have focused on the first hour with maximal anticonvulsive properties of the GYKI 52466.

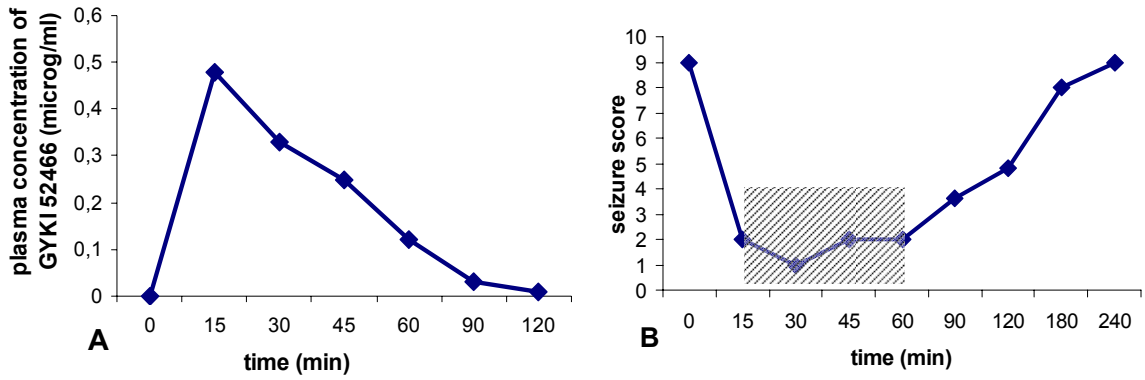

Fig. 14. (A) The time-course of the blood plasma concentration of GYKI 52466. (B) The time-course of the anticonvulsive property of GYKI 52466 (in seizure score; i.e. the higher values indicate more expressed seizure behaviour, therefore lower anticonvulsive effect; *shaded area* indicates the "time frame" for the maximal seizure protection). Modified after *de Sarro et al., 1998*.

5.3 Effect of the pretreatment with glutamate-receptor antagonists on the seizure-associated neuronal activation

MK-801 caused an overall decrease of Fos immunoreactivity, with a staining pattern similar to that observed after dextrometorphan pretreatment (layers II-III, IV, VI, less markedly in layer V) ***(Fig. 5)*** *(Szakács et al, 2003)*. Pretreatment with MK-801 resulted in a significantly lower number of Fos-labelled neurons in CA1, CA2 and CA3 regions of the Ammon's horn with respect to the animals that had received 4-AP only. Pretreatment with MK-801 reduced Fos immunoreactivity in the dentate granule cell layer, as confirmed by statistical evaluation. Moreover, MK-801 resulted in a significant decrease of the number of Fos-containing cell nuclei in the dentate hilus. When given alone, the MK-801 caused only minimal cortical and hippocampal Fos induction. The number of stained cells induced by MK-801 was consistently very low, without significant differences ***(Fig. 10)***.

As for ***GYKI 52466***, to explain the dose-dependent c-fos-IR differences in the neocortex; we presume **(1)** different activity states of the AMPA receptors, depending on the number of modulatory molecules bound by the receptor subunits: GYKI 52466 may act on more binding sites per every subunit, in a concentration-dependent manner *(Arai, 2001)*. In addition to, we also think that **(2)** the lower dose of GYKI 52466 is ineffective in the presence of the high glutamate concentration associated with the early seizure activity *(Kovács et al, 2003)*. The GYKI 52466 seemed to be more effective in delaying the first ictal event, whereas, similarly to some studies, the propagation of the seizure activity *(Barna et al., 2000)* or IEG induction *(Berretta et al., 1997)* seemed to be facilitated in the lower dose pretreatment group. According to the literature *(Hwa and Avoli, 1991; Barna et al., 2000)*, the AMPA receptors are rather involved in the initiation than in the maintenance of seizure (mirrored in our behavioural data for increasing seizure latency and reducing GTCS occurrence); whereas the NMDA receptors play crucial role especially in the

maintenance and propagation of seizure (reflected in the cellular gene expression changes and EM morphology alterations). The majority of the AMPA receptors can be found in the cells of laminae II-III and V-VI *(Sloper and Powell, 1978; Hicks and Conti, 1996)*. The efficacy of the higher dose AMPA antagonism also refers to the importance of AMPAergic excitation in these neocortical strata. The intracortical networks are mainly mediated by NMDA receptors, these connections remain active in spite of the presence of GYKI 52466 *(Barna et al., 2000)*. The induction of 4-AP-induced synchronous network activity in the lower neocortical layers is rather dominated by the excitatory, whilst in the superficial ones, by the inhibitory components *(Yang and Benardo, 2002)*. At the lower dose of GYKI 52466, therefore, we suppose **(3)** a local disequilibrium between the efficacy of AMPA receptor antagonism within the inhibitory population and the overall (rather dominated by the excitatory cells) population, resulting in the overall activation status change reflected by the c-fos-IR differences. The predominance of non-NMDA receptor-mediated excitatory inputs arising from bursting neurons was shown on the fast-spiking GABAergic interneurons *(Hicks and Conti, 1996)*; these cells are also strongly excited by thalamic afferents *(Staiger et al., 1996)*. The inhibitory neurons responsible for surrounding inhibition were less activated under the influence of GYKI 52466 (significant reduction of c-fos expression at higher dose of AMPA receptor antagonist; and showing decreasing trend at lower dose with significant reduction in lamina II). Nevertheless, we found that these interneurons possessed similar AMPA receptor properties to those of the pyramidal cells: the 50 mg/kg dose was needed to significantly decrease the cellular activation. This local balance-shift may also be complicated by the slightly different laminar responses to 4-AP *(Yang and Benardo, 2002)*, since the neocortical PV-containing GABAergic interneurons constitute a heterogeneous population concerning the expression pattern of voltage-gated K^+-channel subunits in the different neocortical laminae *(Chow et al., 1999)*.

In the hippocampal areas studied, even the lower dose (25 mg/kg) of GYKI 52466 was efficient to reduce the *c-fos* immunoreactivity, not only in the parvalbumin-labelled, but also in the whole *c-fos*-IR neuronal population, especially in the granular layer of the dentate gyrus. This fact emphasises the differences in the receptorial distribution and spatial separation of excitatory and inhibitory axon systems in the hippocampus *(McBain et al., 1999; Moga et al., 2002)*. According to immunostaining data, AMPA receptors are concentrated in the outer molecular layer of the dentate gyrus and in the stratum lacunosum-moleculare of the regio superior *(Molnár et al., 1993)*, while NMDA receptors are relatively scarce in the same regions *(Kopniczky et al, 2005).* These layers are the main excitatory input areas: the axon terminals of the perforant path synapse here *(Lado et al., 2002)*. The prominent contribution of the AMPA receptors to the activation of the

neuronal circuits is shown by the significant reduction of the number of the *c-fos*-IR cells of the hippocampal CA1, CA2 and CA3 sectors and in the stratum granulosum and hilus of the dentate gyrus, even by the lower (25 mg/kg) pretreatment dose.

5.4 Effect of the pretreatment with glutamate-receptor antagonists on the seizure-associated pericapillary astrocytic swelling

On the basis of the morphological results, we conclude that acute seizures caused the measurable swelling of the astrocytes *(Kimelberg, 2004)*. Our investigations *(Fabene et al., 2006)* revealed the importance of brain swelling in 4-AP seizures: the long-lasting astrocyte swelling was responsible for the critical decrease of apparent diffusion coefficient (ADC) values, as shown by our MRI experiments. Regional differences in astrocytic swelling *(Fabene et al., 2006)* are likely due to the various astrocytic capacities for glutamate metabolism, neurotransmission *(Bordey and Sontheimer, 2000)* and aquaporin-synthesis *(Han et al., 2004)*. The swelling of the astrocytes *(Kimelberg, 2004)* obliterates brain extracellular spaces, inhibiting the clearance of transmitters, ions and HCO_3^- from the extracellular space; contributing to and enhancing the cellular damage *(Van Gelder, 1983)*; leading to a long-lasting decrease in volume transmission *(Syková, 2005; Fabene et al, 2006)*. The current antiepileptics have been shown to exert their effect on the astrocytes by directly depressing their Ca^{2+}-signalling *(Tian et al., 2005)*. The mechanism of seizure-related astrocyte swelling is likely to be multifactorial *(Olsson et al., 2006)*; such as **(1)** circulatory *(Hong et al., 2004)* and **(2)** metabolic *(Briellmann et al., 2005)* changes due to seizure activity. Alternatively, the astroglial volume-change may be secondary to **(3)** the failure of these cells to manage the consequences of increased neuronal activity (e.g. may also derive from fluid uptake secondary to the extracellular changes accompanying elevated neuronal functioning), thus providing a mechanism reinforcing seizure *per se (Olsson et al., 2006)*. Literature data are limited concerning the roles of AMPA receptor antagonism in the seizure-related pericapillary astrocyte swelling; whilst the action of the NMDA receptor antagonists influencing the glia-to-neuron signalisation processes *(Lalo et al., 2006.)* or the changes of the brain water compartments *(Hantzschel and Andreas, 1998)*, or modulating the pericapillary astrocytic swelling following injuries *(Trout et al., 1995)* or following glutamate-administration *(Bender et al., 1998)* have already been described. The glutamate-induced astrocytic swelling can be moderated with MK-801 *(Bender et al., 1998)*. In accordance with these data, we demonstrated the long-term astrocytic oedema-reducing effect of the MK-801-pretreatment in the 4-AP-induced seizure ***(Fig. 11)***. The capillary area enlargement was

limited to the 3h pretreatment group; this alteration may reflect a short-term perfusion change at the affected sites.

In our ***GYKI 52466*** experiments, the AMPA blockade was completely ineffective to decrease the seizure-related astrocyte swelling – in the neocortex GYKI 52466 even increased the swelling of the astroglia. Other studies *(Lees and Leong, 2001)* also question the protective effect of GYKI 52466 against seizure-related morphological damage, which is a contrasting feature with the anticonvulsant efficacy of this compound *(Borowicz et al., 2001; Gulyás-Kovács et al., 2002)*. On the other hand, the above described results from our laboratory proved that in the same experimental conditions NMDA blockade with ***MK-801*** decreased brain oedema significantly ***(Fig. 11)***, indicating the differences between roles of the ionotropic receptors, and the significance of glutamate. Thus, the overactivation of NMDA receptors is suggested mainly in the background of the morphological changes of the 4-AP paradigm *(Peña and Tapia, 1999)*.

The effects of ***DMSO*** on glutamate responses *(Lu and Mattson, 2001; Tsvyetlynska et al., 2005)* (exerting direct effect on the activity of ionotropic glutamate receptors or neurotransmitter release, possibly by interacting with the channel proteins or modulating the redox state via its antioxidant property) should be taken into account in interpreting the results of experiments in which DMSO is used as a solvent *(Santos et al., 2003)*. DMSO administration (as a drug vehicle) increases the drug concentration into the extracellular space, but since the BBB permeability is increased, it may also provide an avenue for development of vasogenic oedema *(Kleindienst et al., 2006)*. Taken together, the oedematous changes in the pericapillary territories may partially due to the side effects of the vehicle used in this experiment. This point can be hardly clarified without using other vehicles. Other methods for dissolving GYKI 52466, such as using distilled water *(Block et al., 1996)*, physiological saline *(Kubová et al., 1997)*, or acidic solutions titrated back to neutral pH *(Barna et al., 2000)* were proven equally irreproducible in our laboratory. According to the literature *(Lees and Leong, 2001)* and to our experience, as well, GYKI 52466 was insoluble in water, and instable in solutions above pH 4. In our next fMRI and EM experiments 2-hydroxypropyl-β-cyclodextrin (HPCD) *(Jakus et al., 2004)* or CREMOFOR EL *(Berretta et al., 1997)* as a much more inert vehicle than DMSO is planned to be used. Nevertheless, in another GYKI 52466 study, the HPCD elevated the AMPA/kainate toxicity by increasing the amount of seizure damage *(Lees and Leong, 2001)*.

6. CONCLUSIONS

In our pilot study *(Fabene et al., 2006)* we have described the properties of the 4-AP-evoked seizure activity in the rat brain by means of structural and functional MRI. These are ***the first MRI data about the 4-AP acute convulsive model***, providing information for further experiments about the possible treatment options in this rat convulsion paradigm.

On the basis of the above described results, we conclude that seizure-related astrocyte swelling is unlikely to be mediated by AMPA receptors, and ***blockade of the AMPA receptor does not protect against astroglial swelling in epilepsy*** *(Weiczner et al., 2008)*. Further investigation should elucidate the role of astrocytic glutamate receptors in the 4-AP-elicited acute convulsions and the pathophysiology of astrocytic oedema associated with generalised tonic-clonic seizures. In the following experiments, we are going to study the role and proportional involvement of glutamatergic transmission (glial glutamate receptors and transporters) and other cellular factors (such as aquaporins and connexins) in the seizure-associated astrocytic swelling *(Zádor et al., 2008)*. As for comparison, the efficacy of different current antiepileptics will be assessed within the same experimental paradigm.

Summarizing our results, it seems that ***the main protective effect of GYKI 52466 is based on the moderate inhibition of seizure activity only*** (increasing the latency of the GTCS, and decreasing the lethality in the animal groups); although the relatively short duration of action may also have contributed to the limited effects of GYKI 52466. This notion, concerning the low therapeutic index of GYKI 52466, is supported by the literature *(Lees and Leong, 2001; Jakus et al., 2004)*. Our data suggest that ***the seizure-associated cellular damages (such as astrocytic swelling) depend critically rather on the participation of NMDA receptors*** *(Peña and Tapia, 1999; Lado et al., 2002; Zádor et al., 2008)*, than on the AMPA receptors. ***In the hippocampus, cellular activation was rather dependent on AMPA receptors than in the neocortex***, but astrocyte swelling was not. We think therefore, in accordance with the literature *(Berretta et al., 1997; Barna et al., 2000; Jakus et al., 2004)* that the AMPA receptors are rather involved in the initiation, than in the maintenance and propagation of cortical seizure activity. The different extent of participation of AMPA receptors in organising neuronal circuits of neocortex and hippocampus in convulsions is reflected by the dissimilar GYKI 52466 efficacy in reducing the seizure-related neuronal activation. By our experience in the 4-AP convulsion paradigm, rather the antagonists of the NMDA than AMPA receptors play crucial role in circumventing the acute morphological changes, such as astrocytic swelling.

7. ACKNOWLEDGEMENTS

I am indebted to ***Prof. Dr. András Mihály*** (Professor and Chairman of the Department of Anatomy, Histology and Embryology, Faculty of Medicine, University of Szeged) for his professional mentorship, consultative support throughout the elaboration of this thesis and scientific guidance for my research and teaching activities in the Department of Anatomy.

The MRI measurements were performed in the Experimental MRI Laboratory of the Department of Anatomy and Histology, Faculty of Medicine, University of Verona, Verona, Italy. I am indebted to ***Dr. Paolo F. Fabene, Dr. Pasquina Marzola, Prof. Dr. Marina Bentivoglio, Prof. Dr. Andrea Sbarbati, and Prof. Dr. Francesco Osculati*** for their kindness and professional help during my Italian stay.

The examined AMPA receptor antagonist compound (GYKI 52466) was a generous gift of ***Dr. Katalin Horváth***, research manager of the IVAX GYKI Co-Ltd. (Budapest, Hungary).

My thanks are due to my co-author colleague, ***Beáta Krisztin-Péva***, for her professional help in the rough field of the statistical analyses.

The precise technical help from the staff of our Department, namely that of ***Márta Dukai, Gabriella Papp, Katica Lakatos, Mónika Kara, Andrea Kobolák, Ilona Fekete, Tünde Tóth-Németi, Ferenc Rácz*** and ***Zoltán Imre*** (Department of Anatomy, Histology and Embryology, Faculty of Medicine, University of Szeged) is greatly appreciated.

Based on my ideas, Fig. 3 is the design of ***Dr. Csaba Bohata*** and ***Dr. Róbert Fenyő*** (molecule model of 4-AP). I would like to express my gratitude to them.

I have carried out the EM measurements in the EM Laboratory of the Department of Pathology (Faculty of Medicine, University of Szeged). I am grateful to ***Dr. Zsolt Rázga*** and ***Mária Bakacsi*** for providing me the accessibility of the EM apparatus.

Finally, I would like to express my special thanks to ***my family***, and first of all, to ***my wife***, ***Dr. Ágnes Dobi***, whose support and love helped me to overcome the recent stressful and complicated period of my life, and thus enabled me to accomplish my doctoral thesis.

8. REFERENCES

V. **Abekawa**, T., Ito, K., Nakagawa, S., Koyama, T., *2007.* Prenatal exposure to an NMDA receptor antagonist, MK-801 reduces density of parvalbumin-immunoreactive GABAergic neurons in the medial prefrontal cortex and enhances phencyclidine-induced hyperlocomotion but not behavioral sensitization to methamphetamine in postpubertal rats. *Psychopharmacology (Berl). 192(3), 303-316.*

VI. **Alexander**, S. P. H., Peters, J. A., *2000.* Receptor & ion channel nomenclature supplement. *Trends Pharmacol. Sci. 11, 1–120.*

VII. **Amaral**, D. G., *1978.* A Golgi study of cell types in the hilar region of the hippocampus in the rat. *J. Comp. Neurol. 182, 851–914.*

VIII. **Andreani**, A.; Leoni, A.; Locatelli, A.; Morigi, R.; Rambaldi, M.; Pietra, C.; Villetti, G.; *2000.* 4-aminopyridine derivates with antiamnestic activity. *Eur. J. Med. Chem. 35, 77-82.*

IX. **Arai**, A. C.*, 2001.* GYKI 52466 has positive modulatory effects on AMPA receptors. *Brain Res. 892, 396-400.*

X. **Arias**, R. L., Tasse, J. R. P., Bowlby, M. R., *1999.* Neuroprotective interaction effects of NMDA and AMPA receptor antagonists in an in vitro model of cerebral ischemia. *Brain Res. 816, 299-308.*

XI. **Barna**, B., Szász, A., Világi, I., Szente, M., *2000.* Anticonvulsive effect of AMPA receptor antagonist GYKI 52466 on 4-aminopyridine-induced cortical ictal activity in rat. *Brain Res. Bull. 51(3), 241-248.*

XII. **Bender**, A. S., Schousboe, A., Reichelt, W., Norenberg, M. D., *1998.* Ionic mechanisms in glutamate-induced astrocyte swelling: role of K+ influx. *J. Neurosci. Res. 52(3), 307-321.*

XIII. **Berger**, S. G., Waser, P.G., Sin-Ren, A. C., *1989.* Distribution of the 4-aminopyridine derivative 3-methoxy-4-aminopyridine in mice. *Neuropharm. 28 (2), 191-194.*

XIV. **Berretta**, S., Parthasarathy H. B.**,** Graybiel**,** A. M., *1997.* Local release of GABAergic inhibition in the motor cortex induces immediate-early gene expression in indirect pathway neurons of the striatum. *J. Neurosci.17(12), 4752-4763.*

XV. **Biegon**, A., Gibbs, A., Alvarado, M., Ono, M., Taylor, S., *2007.* In vitro and in vivo characterization of [3H]CNS-5161--a use-dependent ligand for the N-methyl-D-aspartate receptor in rat brain. *Synapse 61(8), 577-586.*

XVI. **Blendy**, J. A.; Schmid, W.; Kiessling, M.; Schütz, G.; Gass, P.; *1995.* Effects of kainic acid induced seizures on immediate early gene expression in mice with a targeted mutation of the CREB gene. *Brain Res. 681, 8-14.*

XVII. **Block**, F., Schmitt, W., Schwarz, M., *1996.* Pretreatment but not posttreatment with GYKI 52466 reduces functional deficits and neuronal damage after global ischemia in rats. *J. Neur. Sci. 139, 167-172.*

XVIII. **Block**, F.; Schwarz, M.; *1994.* The depressant effect of GYKI 52466 on spinal reflex transmission in rats is mediated via non-NMDA and benzodiazepine receptors. *Eur. J. Pharmacol. 256(2), 149-153.*

XIX. **Blumenfeld**, H.; *2007.* Functional MRI studies of animal models in epilepsy. *Epilepsia. 48 Suppl. 4, 18-26.*

XX. **Bordey**, A., Sontheimer, H., *2000.* Ion channel expression by astrocytes in situ: comparison of different CNS regions. *Glia 30(1), 27-38.*

XXI. **Borowicz**, K. K., Duda, A. M., Kleinrok, Z., Czuczwar, S. J., *2001.* Interaction of GYKI 52466, a selective non-competitive antagonist of AMPA/kainate receptors, with conventional antiepileptic drugs in amygdala-kindled seizures in rats. *Pol. J. Pharmacol. 53(2), 101-108.*

XXII. **Bremer**, C., Mustafa, M., Bogdanov Jr., A., Ntziachristos, V., Petrovsky, A., Weisseleder, R., *2003.* Steady-state blood volume measurements in experimental tumors with different angiogenic burdens a study in mice. *Radiology 226, 214– 220.*

XXIII. **Briellmann**, R. S., Wellard, R. M., Jackson, G. D., *2005*. Seizure-associated abnormalities in epilepsy: evidence from MR imaging. *Epilepsia 46(5), 760-766.*

XXIV. **Brückner**, C., Heinemann, U., *2000.* Effects of standard anticonvulsant drugs on different patterns of epileptiform discharges induced by 4-aminopyridine in combined entorhinal cortex-hippocampal slices. *Brain Res. 859, 15-20.*

XXV. **Burette**, A., Khatri, L., Wyszynski, M., Sheng, M., Ziff, E. B., Weinberg, R. J., *2001*. Differential cellular and subcellular localization of ampa receptor-binding protein and glutamate receptor-interacting protein. *J. Neurosci. 21(2), 495-503.*

XXVI. **Choe**, E.S., Wang, J.Q., *2002.* Regulation of transcription factor phosphorylation by metabotropic glutamate receptor-associated signaling pathways in rat striatal neurons. *Neuroscience 114, 557–565.*

XXVII. **Chow**, A., Erisir, A., Farb, C., Nadal, M. S., Ozaita, A., Lau, D., Welker, E., Rudy, B., *1999.* K^+ channel expression distinguishes subpopulations of parvalbumin- and somatostatin-containing neocortical interneurons. *J. Neurosci. 19(21), 9332-9345.*

XXVIII. **Clifford**, D. B., Olney, J. W., Benz, A. M., Fuller, T. A., Zorumski, C. F., *1990.* Ketamine, phencyclidine, and MK-801 protect against kainic acid-induced seizure-related brain damage. *Epilepsia 31(4), 382-390.*

XXIX. **Conti**, F.; Weinberg, R. J., *1999.* Shaping excitation at glutamatergic synapses. *TINS 22(10), 451-458.*

XXX. **Czuczwar**, S. J.; Borowicz, K. K.; Kleinrok, Z.; Tutka, P.; Zarnowski, T.; Turski, W. A.; *1995.* Influence of combined treatment with NMDA and non-NMDA receptor antagonists on electroconvulsions in mice. *Eur. J. Pharm. 281, 327-333.*

XXXI. **DeFelipe**, J., *1997*. Types of neurons, synaptic connections and chemical characteristics of cells immunoreactive for calbindin-D28K, Parvalbumin and calretinin in the neocortex. *J. Chem. Neuroanat. 14, 1-19.*

XXXII. **Dóczi**, J.; Banczerowski-Pelyhe, I.; Barna, B.; Világi, I.; *1999.* Effect of a glutamate receptor antagonist (GYKI 52466) on 4-aminopyridine-induced seizure activity developed in rat cortical slices. *Brain Res. Bull. 49(6), 435-440.*

XXXIII. **Donevan**, S. D., Rogawski, M. A., *1998.* Allosteric regulation of α-amino-3-hydroxy-5-methyl-4-isoxazole-propionate receptors by thiocyanate and cyclothiazide at a common modulatory site distinct from that of 2,3-benzodiazepines. *Neurosci. 87, 615-629.*

XXXIV. **Dragunow**, M., Currie, R. W., Faull, R. L. M., Robertson, H. A., Jansen, K., *1989.* Immediate-early-genes, kindling and long-term potentiation. *Neurosci. Behav. Rev. 24, 301–313.*

XXXV. **Dousset,** V., Gomez, C., Petry, K.G., Delalande, C., Caille, J.M., *1999.* Dose and scanning delay using USPIO for central nervous system macrophage imaging. *MAGMA 8, 185–189.*

XXXVI. **Eyjolfsson**, E.M., Brenner, E., Kondziella, D., Sonnewald, U., *2006*. Repeated injection of MK-801: an animal model of schizophrenia? *Neurochem Int. 48(6-7), 541-546.*

XXXVII. **Fabene**, P.F., Marzola, P., Sbarbati, A., Bentivoglio, M., *2003.* Magnetic resonance imaging of changes elicited by status epilepticus in the rat brain: diffusion-weighted and T2-weighted images, regional blood volume maps, and direct correlation with tissue and cell damage. *Neuroimage 18, 375– 389.*

XXXVIII. **Fabene**, P. F., Weiczner, R., Marzola, P., Nicolato, E., Calderan, L., Andrioli, A., Farkas, E., Süle, Z., Mihály, A., Sbarbati, A., *2006*. Structural and functional MRI following 4-aminopyridine-induced seizures: a comparative imaging and anatomical study *Neurobiol. Dis. 21, 80-89.*

XXXIX. **Farkas**, I.G., Czigner, A., Farkas, E., Dobó, E., Soós, K., Penke, B., Endrész, V., Mihály, A., *2003.* Beta-amyloid peptide-induced blood– brain barrier disruption facilitates T-cell entry into the rat brain. *Acta Histochem. 105, 115– 125.*

XL. **Fujikawa**, D. G., Söderfeldt, B., Wasterlain, C. G., *1992.* Neuropathological changes during generalised seizures in newborn monkeys. *Epilepsy Res. 12(3), 243-251.*

XLI. **Gass**, P., Herdegen, T., Bravos, R., Kiessling, M., *1992.* Induction of immediate early gene encoded proteins in the rat hippocampus after bicuculline-induced seizures: Differential expression of KROX-24, fos and jun proteins. *Neurosci. 48, 315–324.*

XLII. **Gebhart**, C.; Breitenbach, U.; Tuckermann, J. P.; Dittrich, B. T.; Richter, K. H.; Angel, P.; *2002.* Calgranulin S100A8 and S100A9 are negatively regulated by glucocorticoids in a c-fos-dependent manner and overexpressed throughout skin carcinogenesis. *Oncogene, 21, 4266-4276.*

XLIII. **van Gelder** N. M., Siatitsas, I., Menini, C., Gloor, P., *1983.* Feline generalized penicillin epilepsy: changes of glutamic acid and taurine parallel the progressive increase in excitability of the cortex. *Epilepsia 24(2), 200-213.*

XLIV. **Grass**, A., Niendorf, T., Hirsch, J.G., *2001.* Acute and chronic changes of the apparent diffusion coefficient in neurological disorders—Biophysical mechanisms and possible underlying histopathology. *J. Neurol. Sci. 186, S15– S23.*

XLV. **Greenberg**, M. E., Ziff, E. B., *2001.* Signal transduction in the postsynaptic neuron. Activity-dependent regulation of gene expression. *In: Cowan, W. M.; Südhof, T. C.; Stevens, C. F., eds. Synapses. Baltimore: The Johns Hopkins University Press; 2001: 357–391.*

XLVI. **Gulyás-Kovács**, A., Dóczi, J., Tarnawa, I., Détári, L., Banczerowski-Pelyhe, I., Világi, I., *2002.* Comparison of spontaneous and evoked epileptiform activity in three in vitro epilepsy models. *Brain Res. 945, 174-180.*

XLVII. **Han**, B. C., Koh, S. B., Lee, E. Y., Seong, Y. H., *2004.* Regional difference of glutamate-induced swelling in cultured rat brain astrocytes. *Life Sci. 76, 573-583.*

XLVIII. **Hantzschel**, A., Andreas, K., *1998.* Efficacy of glutamate receptor antagonists in the management of functional disorders in cytotoxic brain ooedema induced by hexachlorophene. *Pharmacol. Toxicol. 82(2), 80-88.*

XLIX. **Hardingham**, G. E.; Arnold, F. J. L.; Bading, H.; *2001.* Nuclear calcium signalling controls CREB-mediated gene expression triggered by synaptic activity. *Nat. Neurosci. 4 (3), 261-267.*

L. **Hasegawa**, D., Orima, H., Fujita, M., Nakamura, S., Takahashi, K., Ohkubo, S., Igarashi, H., Hashizume, K., *2003.* Diffusion-weighted imaging in kainic acid-induced complex partial status epilepticus in dogs. *Brain Res. 9831-2, 115– 127.*

LI. **Herdegen**, T., Waetzig, V., *2001.* AP-1 proteins in the adult brain: Facts and fiction about effectors of neuroprotection and neurodegeneration. *Oncogene 20, 2424–2437.*

LII. **Herdegen**, T., Leah, J. D., *1998.* Inducible and constitutive transcription factors in the mammalian nervous system: Control of gene expression by Jun, Fos and Krox, and CREB/ATF proteins. *Brain Res. Rev. 28, 370–490.*

LIII. **Hicks**, T. P.; Conti, F.; *1996.* Amino acids as the source of considerable excitation in cerebral cortex. *Can. J. Physiol. Pharmacol. 74, 341–361.*

LIV. **Holtkamp**, M., Meierkord, H., *2007.* Anticonvulsant, antiepileptogenic, and antiictogenic pharmacostrategies. *Cell Mol Life Sci. 64(15), 2023-2041.*

LV. **Hong**, K. S., Cho, Y. J., Lee, S. K., Jeong, S. W., Kim, W. K., Oh, E. J., *2004.* Diffusion changes suggesting predominant vasogenic ooedema during partial status epilepticus. *Seizure 13(5), 317-321.*

LVI. **Hou**, Y-N.; Cebers, G.; Terenius, L.; Liljequist, S.; *1997.* Characterisation of NMDA- and AMPA-induced enhancement of AP-1 DNA binding activity in rat cerebellar granule cells. *Brain Res. 754, 79-87.*

LVII. **Hwa**, G. G. C.; Avoli, M.; *1991.* The involvement of excitatory amino acids in neocortical epileptogenesis: NMDA and non-NMDA receptors. *Exp. Brain Res. 186, 248–256.*

LVIII. **Jakus**, R., Gráf, M., Andó, R. D., Balogh, B., Gacsályi, I., Lévay, G., Kántor, S., Bagdy, G. E., *2004*. Effect of two noncompetitive AMPA receptor antagonists GYKI 52466 and GYKI 53405 on vigilance, behavior and spike-wave discharges in a genetic rat model of absence epilepsy. *Brain Res. 1008(2), 236-244.*

LIX. **Jones**, E. G.; Heron, J. R.; Foster, D. H.; Snelgar, R. S.; Mason, R.; *1983.* Effects of 4-aminopyridine in patients with multiple sclerosis. *J. Neur. Sci. 60, 353-362.*

LX. **Kelso**, A. R. C., Cock, H. R., *2004*. Advances in epilepsy. *Brit. Med. Bull. 72, 135-148.*

LXI. **Kimelberg**, H. K., *2004.* Water homeostasis in the brain: basic concepts. *Neurosci. 129, 851-860.*

LXII. **Kleindienst**, A.; Dunbar, J. G.; Glisson, R.; Okuno, K.; Marmarou, A.; *2006.* Effect of dimethyl sulfoxide on blood-brain barrier integrity following middle cerebral artery occlusion in the rat. *Acta Neurochir. Suppl. 96, 258-262.*

LXIII. **Kopniczky**, Z., Dobó, E., Borbély, S., Világi, I., Détári, L., Krisztin-Péva, B., Bagosi, A., Molnár, E., Mihály, A., *2005.* Lateral entorhinal cortex lesions rearrange afferents, glutamate receptors, increase seizure latency and suppress seizure-induced c-fos expression in the hippocampus of adult rat. *J. Neurochem. 95(1), 111-124.*

LXIV. **Kovács**, A., Mihály, A., Komáromi, Á., Gyengési, E., Szente, M., Weiczner, R., Krisztin-Péva, B., Szabó, Gy., Telegdy, Gy., *2003.* Seizure, neurotransmitter release, and gene expression are closely related in the striatum of 4-aminopyridine-treated rats. *Epil. Res. 55, 117-129.*

LXV. **Kubová**, H.; Világi, I.; Mikulecká, A.; Mareš, P.; *1997.* Non-NMDA receptor antagonist GYKI 52466 suppresses cortical afterdischarges in immature rats. *Eur. J. Pharm. 333, 17-26.*

LXVI. **Labiner**, D. M., Butler, L. S., Cao, Z., Hosford, D. A., Shin, C., McNamara, J. O., *1993.* Induction of c-*fos* mRNA by kindled seizures: Complex relationship with neuronal burst firing. *J. Neurosci. 1, 744–751.*

LXVII. **Lado**, F. A., Laureta, E. C., Moshé, S. L., *2002*. Seizure-induced hippocampal damage in the mature and immature brain. *Epil. Disord. 4(2), 83-97.*

LXVIII. **Lalo**, U., Pankratov, Y., Kirchhoff, F., North, R.A., Verkhratsky, A., *2006.* NMDA receptors mediate neuron-to-glia signaling in mouse cortical astrocytes. *J Neurosci. 26(10): 2673-2683*.

LXIX. **Lees**, G. J., Leong, W., *2001.* In vivo, the direct and seizure-induced neuronal cytotoxicity of kainate and AMPA is modified by the non-competitive antagonist, GYKI 52466. *Brain Res. 890, 66-77.*

LXX. **Lemeignan**, M., Millart, H., Lamiable, D., Molgo, J., Lechat, P., *1984.* Evaluation of 4-aminopyridine and 3,4-diaminopyridine penetrability into cerebrospinal fluid in anesthetized rats. *Brain Res. 304, 166-169.*

LXXI. **Lojková**, D., Zivanović, D., Mares, P., 2006. Different effects of nonNMDA and NMDA receptor antagonists (NBQX and dizocilpine) on cortical epileptic afterdischarges in rats. *Brain Res. 1124(1), 167-175.*

LXXII. **Lu**, C.; Mattson, M. P.; *2001*. Dimethyl sulfoxide suppresses NMDA- and AMPA-induced ion currents and calcium influx and protects against excitotoxic death in hippocampal neurons. *Exp. Neurol. 170(1), 180-185.*

LXXIII. **Lukasiuk**, K., Pitkänen, A., *2000.* $GABA_A$-mediated toxicity of hippocampal neurons in vitro. *Journ. Neurochem. 74(6), 2445-2453.*

LXXIV. **Mandeville**, J.B., Marota, J.J., Kosofsky, B.E., Keltner, J.R., Weissleder, R., Rosen, B.R., Weisskoff, R.M., *1998.* Dynamic functional imaging of relative cerebral blood volume during rat forepaw stimulation. *Magn Reson Med 39, 615–624.*

LXXV. **McBain**, C. J., Freund, T. F., Mody, I., *1999.* Glutamatergic synapses onto hippocampal interneurons: precision timing without lasting plasticity. *TINS 22(5), 228-235.*

LXXVI. **Meldrum**, B. S., Rogawski M. A., *2007*. Molecular targets for antiepileptic drug development. *Neurotherap 4(1): 18–61.*

LXXVII. **Mihály**, A., Bencsik, K., Solymosi, T., *1990.* Naltrexone potentiates 4-aminopyridine seizures in the rat. *J. Neural. Transm. (GenSect) 79, 59–67.*

LXXVIII. **Mihály**, A., Borbély, S., Világi, I., Détári, L., Weiczner, R., Zádor, Zs., Krisztin-Péva, B., Bagosi, A., Kopniczky, Zs., Zádor, E., *2005.* Neocortical c-fos mRNA transcription in repeated, brief, acute seizures: Is c-fos a coincidence detector? *Int. J. Mol. Med. 15, 481-486.*

LXXIX. **Mihály**, A., Szakács, R., Bohata, Cs., Dobó , E., Krisztin-Péva, B., *2001.* Time-dependent distribution and neuronal localization of c-fos protein in the rat hippocampus following 4-aminopyridine seizures. *Epilepsy Res. 44, 97– 108.*

LXXX. **Moga**, D., Hof, P. R., Vissavajjhala, P., Moran, T. M., Morrison, J. H., *2002.* Parvalbumin-containing interneurons in rat hippocampus have an AMPA receptor profile suggestive of vulnerability to excitotoxicity. *J. Chem. Neuroanat.*, *23 (4)*, *249-253.*

LXXXI. **Molnár**, E., Baude, A., Richmond, S.A., Patel, P.B., Somogyi, P., McIlhinney R. A. J., *1993.* Biochemical and immunocytochemical characterization of antipeptide antibodies to a cloned GluR1 glutamate receptor subunit: cellular and subcellular distribution in the rat forebrain. *Neuroscience 53: 307-326.*

LXXXII. **Morgan**, J. I., Curran, T., *1991.* Proto-oncogene transcription factors and epilepsy. *TIPS 12, 343-349.*

LXXXIII. **Nusser**, Z.; *2000*. AMPA and NMDA receptors: similarities and differences in their synaptic distribution. *Curr. Opin. Neurobiol. 10, 337-341.*

LXXXIV. **Obrenovitch**, T. P.; Urenjak, J.; *1997.* Altered glutamatergic transmission in neurological disorders: from high extracellular glutamate to excessive synaptic efficacy. *Prog. In Neurobiol. 51, 39-87.*

LXXXV. **Olsson**, T., Broberg, M., Pope, K. J., Wallace, A, Mackenzie, L., Blomstrand, F., Nilsson, M., Willoughby, J. O., *2006.* Cell swelling, seizures and spreading depression: an impedance study. *Neurosci. 140(2), 505-515.*

LXXXVI. **Papadopoulos**, M. C., Verkman, A. S., *2007.* Aquaporin-4 and brain oedema. *Pediatr. Nephrol. 22, 778-784.0*

LXXXVII. **Paternain**, A. V., Morales, M., Lerma, J., *1995.* Selective antagonism of AMPA receptors unmasks kainate receptor-mediated responses in hippocampal neurons. *Neuron. 14, 185-189.*

LXXXVIII. **Paxinos**, G., Watson, C., *1998.* The rat brain in stereotaxic coordinates. *Academic Press, San Diego.*

LXXXIX. **Peña**, F., Tapia, R., *1999.* Relationships among seizures, extracellular amino acid changes, and neurodegeneration induced by 4-aminopyridine in rat hippocampus. A microdialysis and electro-encephalographic study. *Journ. Neurochem. 72, 2006-2014.*

XC. **Peña**, F., Tapia, R., *2000.* Seizures and neurodegeneration induced by 4-aminopyridine in rat hippocampus *in vivo*: Role of glutamate- and GABA-mediated neurotransmission and of ion channels. *Neuroscience 101, 547–561.*

XCI. **Perkinton**, M. S.; Sihra, T. S.; Williams, R. J.; *1999.* Ca^{2+}-permeable AMPA receptors induce phosphorylation of cAMP response element-binding protein through a phosphatidylinositol 3-kinase-dependent stimulation of the mitogen-activated protein kinase signalling cascade in neurons. *Journ. Neurosci. 19(14), 5861-5874.*

XCII. **Perrault**, P., Avoli, M., *1991.* Physiology and pharmacology of epileptiform activity induced by 4-aminopyridine in rat hippocampal slices. *J. Neurophysiol. 65, 771–779.*

XCIII. **Pisani**, A., Bonsi, P., Catania, M.V., Giuffrida, R., Morari, M., Marti, M., Centonze, D., Bernardi, G., Kingston, A.E., Calabresi, P., *2002*. Metabotropic glutamate 2 receptors modulate synaptic inputs and calcium signals in striatal cholinergic interneurons. *J. Neurosci. 22, 6176–6185.*

XCIV. **Retchkiman**, I., Fischer, B., Platt, D., Wagner, A. P., *1996.* Seizure induced c-fos mRNA in the rat brain: comparison between young and aging animals. *Neurobiol. Aging. 17(1), 41-44.*

XCV. **Rocha**, L., Ondarza, R., Kaufman, D. L., *1999.* Antisense oligonucleotides to c-fos reduce postictal seizure susceptibility following fully kindled seizures in rats. *Neurosci. Lett. 268, 143-146.*

XCVI. **Santos**, N. C.; Figueira-Coelho, J.; Martins-Silva, J.; Saldanha, C.; *2003*. Multidisciplinary utilization of dimethyl sulfoxide: pharmacological, cellular, and molecular aspects. *Biochem. Pharmacol. 65(7), 1035-1041.*

XCVII. **de Sarro**, G., Chimirri, A., de Sarro, A., Gitto, R., Grasso, S., Giusti, P., Chapman, A. G., *1995.* GYKI 52466 and related 2,3-benzodiazepines as anticonvulsant agents in DBA/2 mice. *Eur. J. Pharm. 294, 411-422.*

XCVIII. **de Sarro**, G., Rizzo, M., Sinopoli, V. A., Gitto, R., de Sarro, A., Zappala, M., Chimirri, A., *1998.* Relationship between anticonvulsant activity and plasma level of some 2,3-benzodiazepines in genetically epilepsy-prone rats. *Pharm. Biochem. Behav. 61, 215-220.*

XCIX. **Schmoll**, H., Badan, I., Fischer, B., Wagner, A. P., *2001.* Dynamics of gene expression for immediate early- and late genes after seizure activity in aged rats. *Arch. Ger. & Ger. 32, 199-218.*

C. **Schwaller**, B., Tetko, I. V., Tandon, P., Silveira, D. C., Vreugdenhil, M., Henzi, T., Potier, M. C., Celio, M. R., Villa, A. E. P., *2004.* Parvalbumin deficiency affects network properties resulting in increased susceptibility to epileptic seizures. *Mol. Cell. Neurosci. 25, 650-663.*

CI. **Simard**, M., Nedergaard, M., *2004.* The neurobiology of glia in the context of water and ion homeostasis. *Neurosci 129, 877– 896.*

CII. **Sloper**, J. J., Powell, T. P. S., *1978.* An experimental electron microscope study of afferent connections to the primate motor and somatic sensory cortices. *Phil. Trans. R. Soc. Lond. B. 285, 199-226.*

CIII. **Spyker**, D. A.; Lynch, C.; Shabanowitz, J.; Sinn, J. A.; *1980.* Poisoning with 4-aminopyridine: Report of three cases. *Clin. Tox. 16, 487-497.*

CIV. **Staiger**, J.F., Zilles, K., Freund T., 1996. Distribution of GABAergic elements postsynaptic to ventroposteromedial thalamic projections in layer IV of rat barrel cortex. *Eur. J. Neurosci. 8, 2273-2285.*

CV. **Syková**, E., *2004.* Extrasynaptic volume transmission and diffusion parameters of the extracellular space. *Neurosci 129, 861–876.*

CVI. **Syková**, E., *2005.* Glia and volume transmission during physiological and pathological states. *J. Neur. Transm. 112(1), 137-147.*

CVII. **Szabados**, T., Gigler, G., Gacsályi, I., Gyertyán, I., Lévay, Gy., *2001.* Comparison of anticonvulsive and acute neuroprotective activity of three 2,3-benzodiazepine compounds, GYKI 52466, GYKI 53405, GYKI 53655. *Brain Res. Bull. 55(3), 387-391.*

CVIII. **Szakács**, R., Weiczner, R., Mihály, A., Krisztin-Péva, B., Zádor, Zs., Zádor E., *2003.* Non-competitive NMDA receptor antagonists moderate seizure-induced *c-fos* expression in the rat cerebral cortex. *Brain Res. Bull. 59, 485-493.*

CIX. **Székely**, J. I., Kedves, R., Máté, I., Török, K., Tarnawa, I., *1997.* Apparent antinociceptive and anti-inflammatory effects of GYKI 52466. *Eur. J. Pharm. 336, 143-154.*

CX. **Tarnawa,** I.; Farkas, S.; Berzsenyi, P.; Pataki, A.; Andrási, F.; *1989*. Electrophysiological studies with a 2,3-benzodiazepine muscle relaxant: GYKI 52466. *Eur. J. Pharmacol. 167(2), 193-9*.

CXI. **Tarnawa**, I.; Molnár, P.; Gaál, L.; Andrási, F.; *1992.* Inhibition of hippocampal field potentials by GYKI 52466 in vitro and in vivo. *Acta Physiol Hung. 79(2), 163-9.*

CXII. **Tian**, G. F., Azmi, H., Takano, T., Xu, Q., Peng, W., Lin, J., Oberheim, N., Lou, N., Wang, X., Zielke, H. R., Kang, J., Nedergaard, M., *2005.* An astrocytic basis of epilepsy. *Nat. Med. 11(9), 973-981.*

CXIII. **Trout**, J. J., Lu, C. Y., Goldstone, A. D., Sahgal, S., *1995.* Polyamines and NMDA receptors modulate pericapillary astrocyte swelling following cerebral cryo-injury in the rat. *J. Neurocytol. 24(5), 341-346.*

CXIV. **Tsvyetlynska**, N. A.; Hill, R. H.; Grillner, S.; *2005*. Role of AMPA receptor desensitization and the side effects of a DMSO vehicle on reticulospinal EPSPs and locomotor activity. *J. Neurophysiol. 94(6), 3951-3960.*

CXV. **Versteeg**, D. H. G., Heemskerk, F. M. J., Spieremburg, H. A., Degraan, P. N. E., Schrama, L. H., *1995.* 4-Aminopyridine differentially affects the spontaneous release of radiolabelled transmitters from rat hippocampal slices. *Brain Res. 686, 233–238.*

CXVI. **Weiczner,** R., Krisztin-Péva, B., Mihály, A., *2008.* Blockade of AMPA-receptors attenuates 4-aminopyridine seizures, decreases the activation of inhibitory neurons but is ineffective against seizure-related astrocytic swelling *Epil Res 78(1): 22-32.*

CXVII. **Yang**, L., Benardo, L. S., *2002.* Laminar properties of 4-aminopyridine-induced synchronous network activities in rat neocortex. *Neurosci. 111 (2), 303-313.*

CXVIII. **Zádor**, Zs., Weiczner, R., Mihály, A., *2008.* Long-lasting dephosphorylation of connexin 43 in acute seizures is regulated by NMDA receptors, in the cerebral cortex of the rat *Mol Med Rep Mol Med Rep 5 (1): 721-727.*

CXIX. **Ziołkowska**, B.; Przewłocka, B.; Mika, J.; Łabuz, D.; Przewłocki, R.; *1998.* Evidence for Fos involvement in the regulation of proenkephalin and prodynorphin gene expression in the rat hippocampus. *Molec. Brain Res. 54, 243-251.*

CXX. **Zirpel**, L.; Janowiak, M. A.; Veltri, C. A.; Parks, T. N.; *2000.* AMPA receptor-mediated, calcium-dependent CREB phosphorylation in a subpopulation of auditory neurons surviving activity deprivation. *J. Neurosci. 20(16), 6267-6275.*

9. APPENDIX: COPIES OF *IN EXTENSO* PAPERS RELATED TO THE THESIS

I. Szakács, R., **Weiczner, R.**, Mihály, A., Krisztin-Péva, B., Zádor, Zs., Zádor, E.: Non-competitive NMDA receptor antagonists moderate seizure-induced *c-fos* expression in the rat cerebral cortex. *Brain Res Bull 59: 485-493, 2003*

II. Kovács, A., Mihály, A., Komáromi, Á., Gyengési E., Szente, M., **Weiczner**, **R.,** Krisztin-Péva, B., Szabó, Gy., Telegdy, Gy.: Seizure, neurotransmitter release, and gene expression are closely related in the striatum of 4-aminopyridine-treated rats. *Epil Res 55: 117-129, 2003*

III. Mihály, A., Borbély, S., Világi, I., Détári, L., **Weiczner, R.**, Zádor, Zs., Krisztin-Péva, B., Bagosi, A., Kopniczky, Zs., Zádor, E.: Neocortical c-fos mRNA transcription in repeated, brief, acute seizures: Is *c-fos* a coincidence detector? *Internat J Mol Med 15(3): 481-486, 2005*

IV. Fabene, P. F., **Weiczner, R.**, Marzola, P., Nicolato, E., Calderan, L., Andrioli, A., Farkas, E., Süle, Z., Mihály, A., Sbarbati, A.: Structural and functional MRI following 4-aminopyridine-induced seizures: a comparative imaging and anatomical study *Neurobiol Dis 21: 80-89, 2006*

V. **Weiczner, R.**, Krisztin-Péva, B., Mihály, A.: Blockade of AMPA-receptors attenuates 4-aminopyridine seizures, decreases the activation of inhibitory neurons but is ineffective against seizure-related astrocytic swelling *Epil Res 78(1): 22-32, 2008*

VI. Zádor, Zs., **Weiczner, R**, Mihály, A.: Long-lasting dephosphorylation of connexin 43 in acute seizures is regulated by NMDA receptors, in the cerebral cortex of the rat *Mol Med Rep 5(1): 721-727, 2008*